REPORT DOCUMENTATION PAGE

Form Approved OMB No. 0704-0188

1. REPORT DATE *(DD-MM-YYYY)*	2. REPORT TYPE	3. DATES COVERED *(From - To)*
	Technical Papers	

4. TITLE AND SUBTITLE

5a. CONTRACT NUMBER

5b. GRANT NUMBER

5c. PROGRAM ELEMENT NUMBER

6. AUTHOR(S)

5d. PROJECT NUMBER
2303

5e. TASK NUMBER
M2C8

5f. WORK UNIT NUMBER

7. PERFORMING ORGANIZATION NAME(S) AND ADDRESS(ES)

Air Force Research Laboratory (AFMC)
AFRL/PRS
5 Pollux Drive
Edwards AFB CA 93524-7048

8. PERFORMING ORGANIZATION REPORT

9. SPONSORING / MONITORING AGENCY NAME(S) AND ADDRESS(ES)

Air Force Research Laboratory (AFMC)
AFRL/PRS
5 Pollux Drive
Edwards AFB CA 93524-7048

10. SPONSOR/MONITOR'S ACRONYM(S)

11. SPONSOR/MONITOR'S NUMBER(S)

12. DISTRIBUTION / AVAILABILITY STATEMENT

Approved for public release; distribution unlimited.

13. SUPPLEMENTARY NOTES

14. ABSTRACT

1121 036

15. SUBJECT TERMS

16. SECURITY CLASSIFICATION OF:			17. LIMITATION OF ABSTRACT	18. NUMBER OF PAGES	19a. NAME OF RESPONSIBLE PERSON
a. REPORT	b. ABSTRACT	c. THIS PAGE			Leilani Richardson
Unclassified	Unclassified	Unclassified	A		19b. TELEPHONE NUMBER *(include area code)* (661) 275-5015

62 separate items are enclosed

TP-FY99-0107

✓ Spreadsheet
✓ DTS

MEMORANDUM FOR PRR (In-House Publication)

24 May 1999

FROM: PROI (TI) (STINFO)

SUBJECT: Authorization for Release of Technical Information, Control Number: AFRL-PR-ED-TP-FY99-0107
Bill Larson, "Identification and Condensation of Cyclic C_6 and Cyclic C_8 in Solid Argon and Matrix-Isolated Boron/Carbon"

Presentation **(Public Release)**

Identification and condensation of cyclic C_6 and cyclic C_8 in solid argon

Characterization of matrix isolated B_JC_{n-J} J=0, 1, 2; n=3-11 in solid argon

C. William Larson
Propulsion Directorate
Air Force Research Laboratory
Edwards AFB, CA 93524-7680

HEDM RESEARCH GROUP
Pat Carrick (Chief), Jeff Sheehy (Group Leader), Greg Drake, Hi Young Yoo, Jeffrey Mills, Jerry Boatz, Jessica Harper, Karl Christe, Mario Fajardo, Michael Tinnirello, Michelle DeRose, Paul Jones, Txomin Presilla (Schafer Corporation), Peter Langhoff, Simon Tam, Suresh Suri, William Wilson

University of Florida
Department of Chemistry
Gainesville, Florida
June 8, 1999

Rocket Science

$$\frac{m_{final}}{m_{initial}} = \exp -\frac{\Delta V}{gI_{sp}}$$

$$I_{sp} = \frac{1}{g}\sqrt{2(h_{propellant} - h_{exit})}$$

h = enthalpy per unit mass

SSME

Rockwell International
Rocketdyne Division

SPACE SHUTTLE MAIN ENGINE

The Space Shuttle Main Engine (SSME) was developed expressly for use on America's Space Shuttle. Using a mixture of liquid oxygen and liquid hydrogen, the SSME can attain a maximum thrust level (in vacuum) of 512,300 pounds at 109% power level. The regeneratively cooled engine also features high performance turbopumps for propellant and oxidizer that develop 77,310 horsepower and 29,430 horsepower, respectively. Ultra-high-pressure operation of the pumps and combustion chamber allows expansion of all hot gases through a high-area-ratio exhaust nozzle to achieve efficiencies never previously attained in a production rocket engine. These advantages allow a heavier payload to be carried without increasing launch vehicle size.

SPACE SHUTTLE MAIN ENGINE PERFORMANCE (FULL POWER LEVEL)

Maximum Thrust: (109% Power Level)
- At Sea Level ..... 408,750 pounds
- In Vacuum ..... 8,390 kN ..... 512,300 pounds
- Throttle Range 65%–109%

Pressures:
- Hydrogen Pump Discharge ..... 7,040 psia
- Oxygen Pump Discharge ..... 8,070 psia
- Chamber Pressure ..... 3,260 psia

Specific Impulse (In Vacuum) ..... 4,444 m/s ..... 453.5 seconds

Power: 5.07 GW (Exhaust, in vacuum)

High Pressure Pumps
- Hydrogen ..... 77,310 horsepower
- Oxygen ..... 29,430 horsepower

Area Ratio 77.5:1

Weight: ..... 6.367 x 10⁻⁷ kN/W ..... 6,990 pounds

Mixture Ratio (O/F) 6.0:1

Dimensions: ..... 168 in. long/96 in. wide

Propellants:
- Fuel ..... Liquid Hydrogen
- Oxidizer ..... Liquid Oxygen

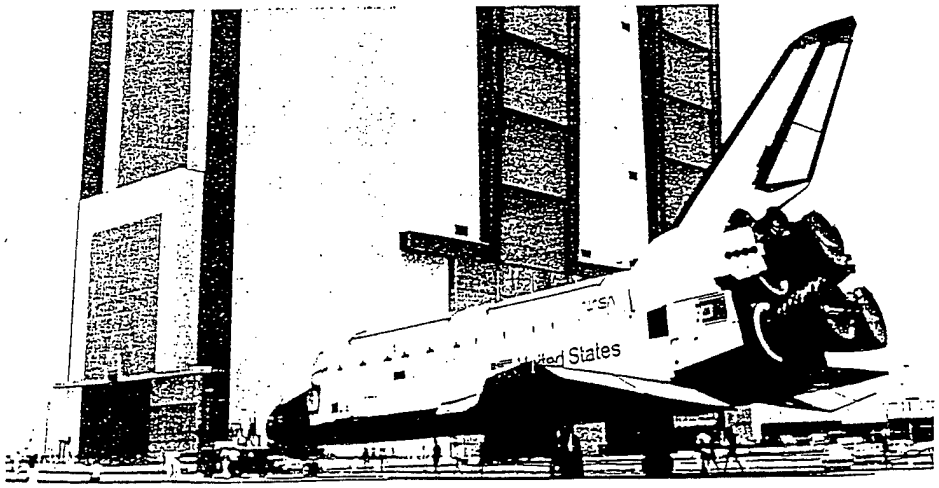

For more information contact: ELV Propulsion/Rockwell International/Rocketdyne Division/6633 Canoga Ave./ Canoga Park/CA/91303/(818)700-6027

Pub. 571-M-80b New 1-7

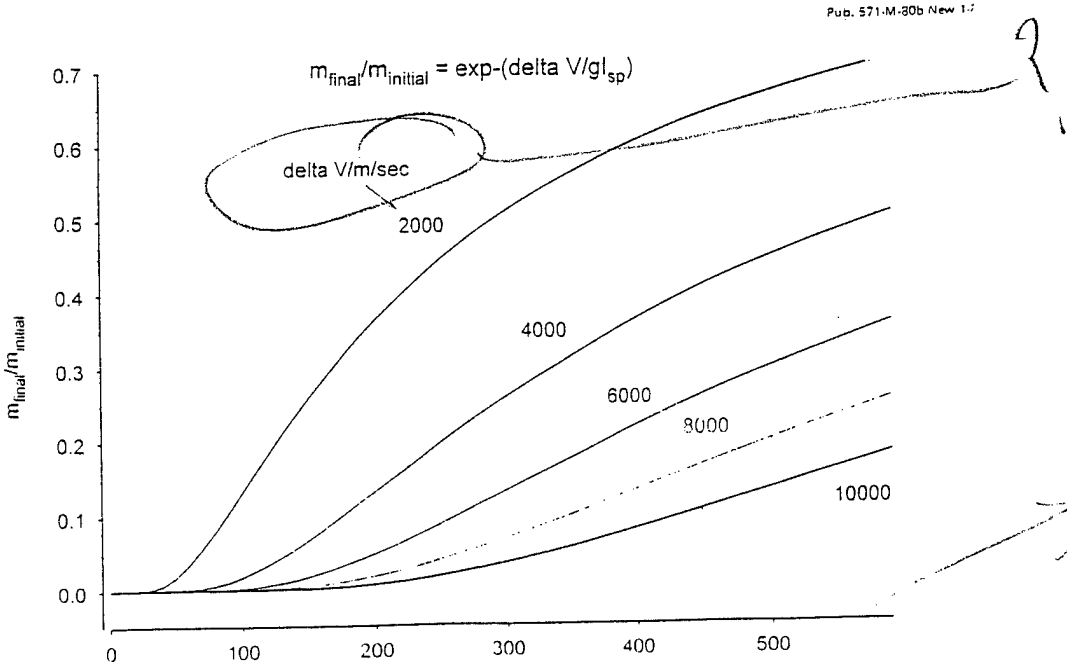

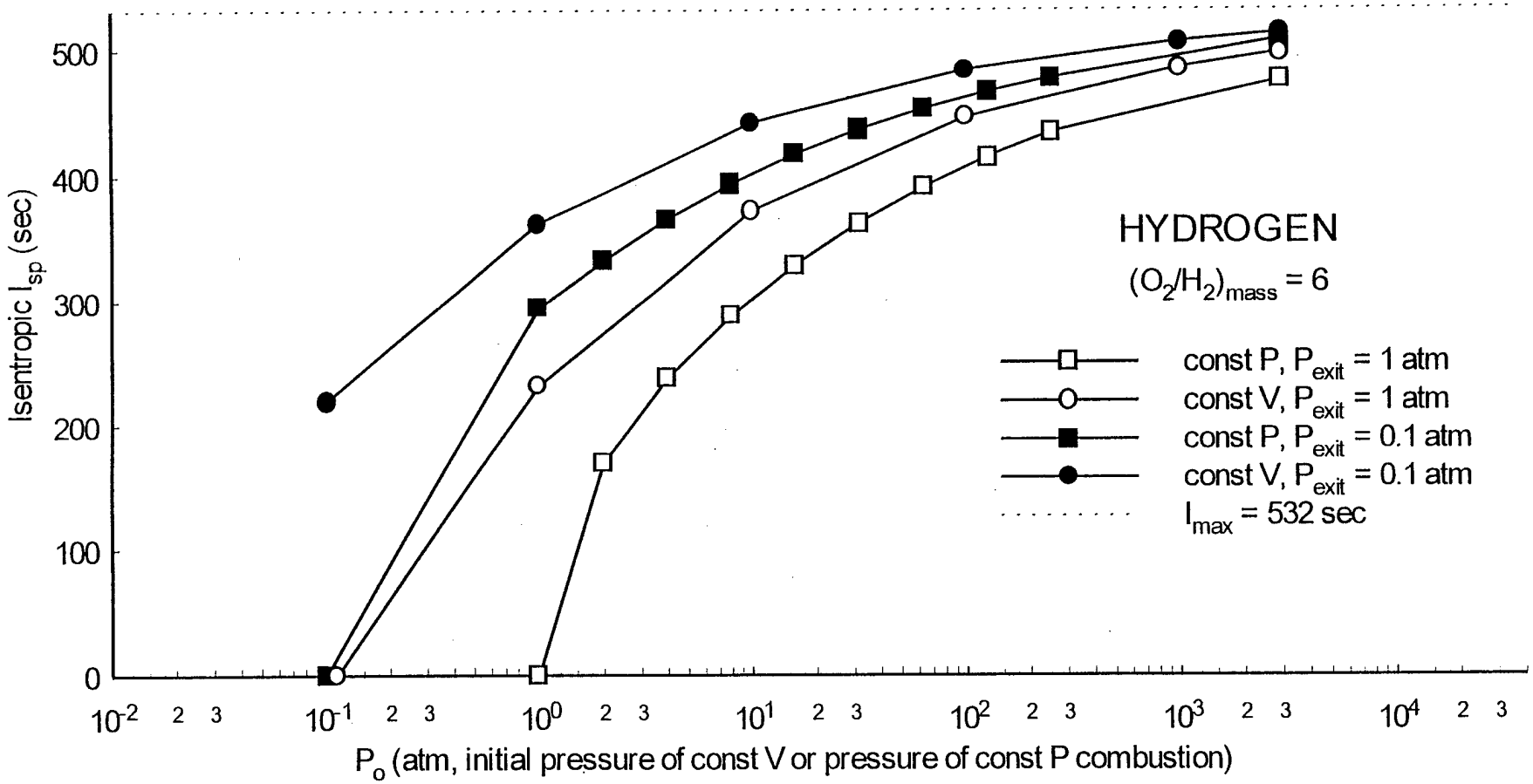
HYDROGEN
$(O_2/H_2)_{mass}$ = 6
const P, P_{exit} = 1 atm
const V, P_{exit} = 1 atm
const P, P_{exit} = 0.1 atm
const V, P_{exit} = 0.1 atm
I_{max} = 532 sec
Isentropic I_{sp} (sec)
P_o (atm, initial pressure of const V or pressure of const P combustion)
0
100
200
300
400
500
10^{-2} 2 3
10^{-1} 2 3
10^{0} 2 3
10^{1} 2 3
10^{2} 2 3
10^{3} 2 3
10^{4} 2 3

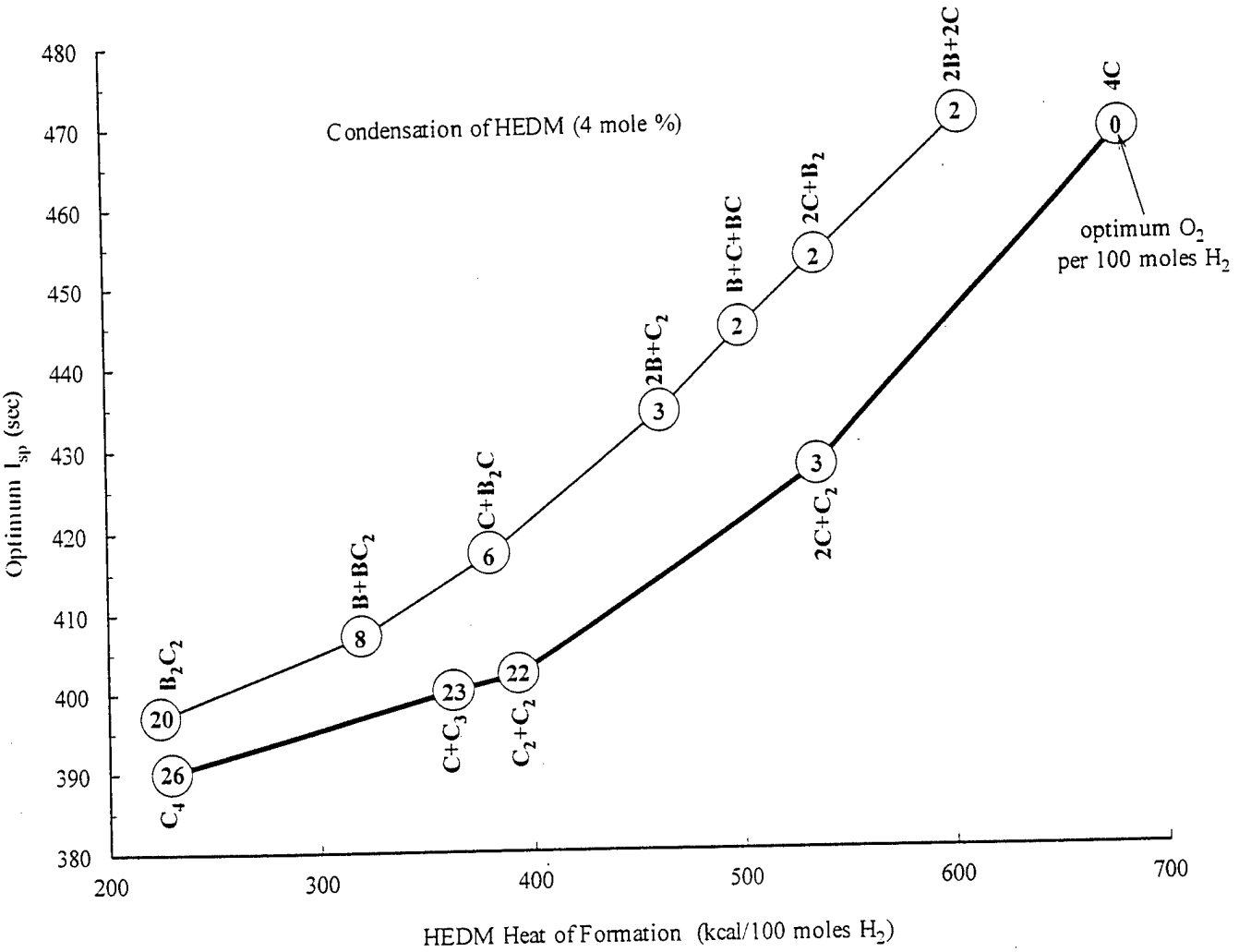

Figure 1. Specific impulse of HEDM containing 4 mole percent equivalent atom density in solid hydrogen with various stages of condensation. Numbers inside circles denote the optimum moles of O_2 per 100 moles of H_2 that produces the maximum Isp for the indicated compositions. The calculations are based on the standard rocket operating conditions, 1000 psi combustion pressure and 1 atm nozzle exit pressure, which produce 389 sec with liquid oxygen/liquid hydrogen propellant. The propellant composed of 4 mole percent C-atoms produces maximum Isp with no oxygen. If the atoms condense to 1 mole percent C4, the Isp drops to the baseline 389 sec value.

Objective - 5% atoms in cryogenic matrix

Approach

1. FTIR spectroscopy of B_JC_{n-J} clusters isolated in 10 K argon matrix

2. Ab-initio calculations of cluster
   (a) normal mode frequencies and frequency shifts of their isotopomers
   (b) infrared absorption intensities (km mol^{-1})

3. Measurement of cluster distributions produced upon deposition and after annealing. Absolute column densities (molecules cm^{-2}) from Beer's Law

$$\langle \rho_i l \rangle = \frac{A_{exp}}{I_{theory}} N$$

$$A_{exp} = -\int_{\nu} \ln\left[\frac{E_t(\nu)}{E_0(\nu)}\right] d\nu$$

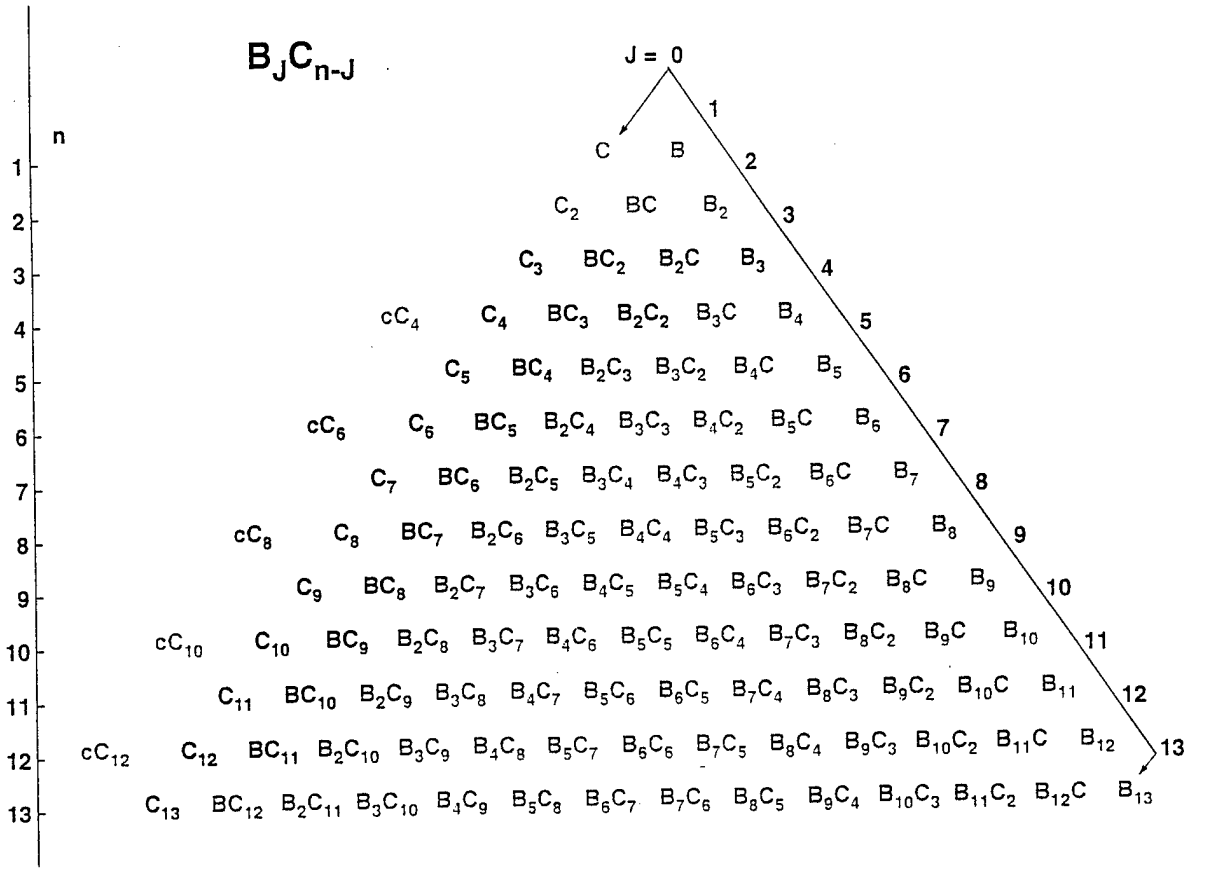

BCSyst2.axg May 13, 1999 2:47:09 PM

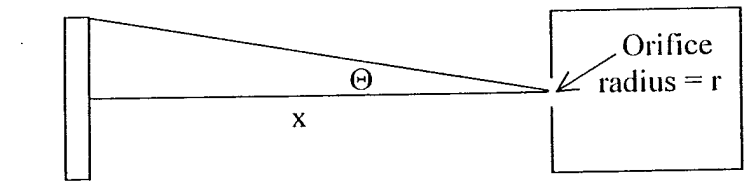

(1) $$Q_{atom}(\Theta, x) = \frac{1}{4}\rho \bar{c}\, a \frac{\cos^3\Theta}{\pi x^2}$$

(2) $$Q_{rad}(\Theta, x) = \sigma T^4 a \frac{\cos^3\Theta}{\pi x^2}$$

Table I. Properties of a boron evaporation oven[(a)], r = 0.05 cm, θ = 0

	x = 10 cm			x = 20 cm
P (Torr)	0.01	0.1	1	10
T (K)	2409	2631	2898	3230
ρ (#/cm^3)	4.01 x 10^{13}	3.67 x 10^{14}	3.33 x 10^{15}	2.98 x 10^{16}
$\bar{c}$ (cm/s)	2.13 x 10^5	2.24 x 10^5	2.35 x 10^5	2.48 x 10^5
Evap rate (#/s)	1.68 x 10^{16}	1.61 x 10^{17}	1.53 x 10^{18}	1.45 x 10^{19}
Evap rate (mg/hour)	1.11	10.6	101	957
λ (cm)[(b)]	100.0	10.9	1.20	0.134
Kn = λ/2r	1000	109	12.0	1.34
Q_{atom} (#/cm^2 s)	5.37 x 10^{13}	5.13 x 10^{14}	4.89 x 10^{15}	1.17 x 10^{16}
Q_{rad} (mW/cm^2)	4.74	6.75	9.93	3.78

(a) Based on vapor pressure data from Nesmeyanov's (1963) compilation, "Vapor Pressure of the Elements."
(b) Mean free path based on a collision diameter of 1.59 x 10^{-8} cm for boron + boron [Moelwyn-Hughes (1961), p25].

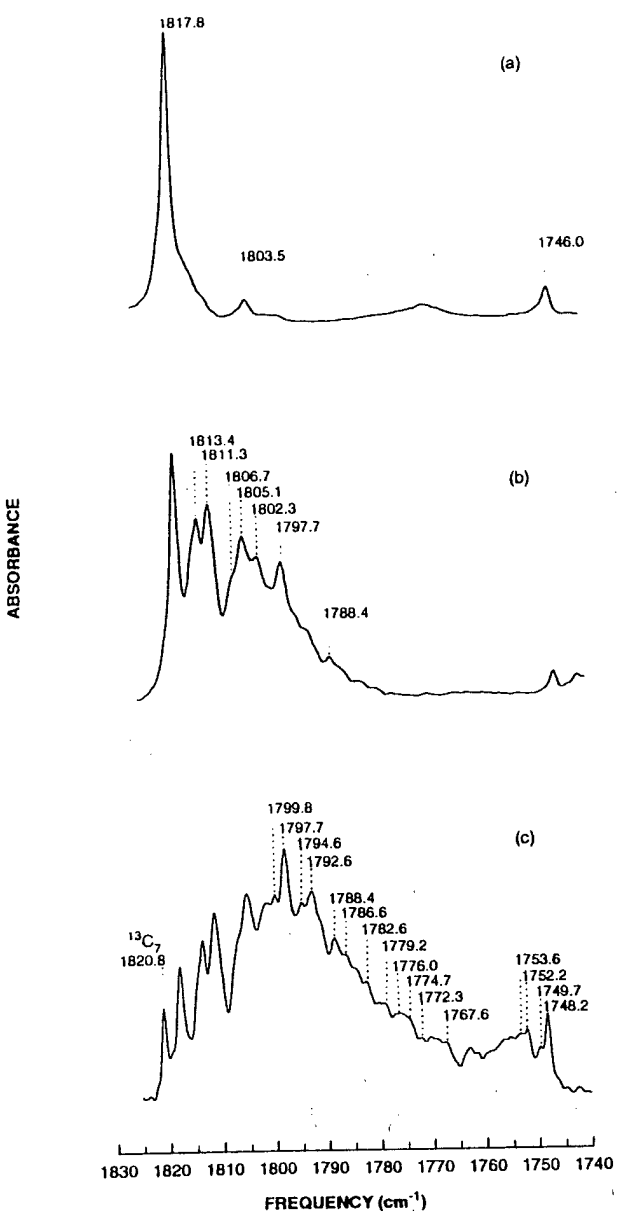
1817.8
(a)
1803.5
1746.0
1813.4
1811.3
1806.7
1805.1
1802.3
1797.7
(b)
1788.4
1799.8
1797.7
1794.6
1792.6
(c)
1788.4
1786.6
1782.6
1779.2
1776.0
1774.7
1772.3
1767.6
$^{13}C_7$
1820.8
1753.6
1752.2
1749.7
1748.2
ABSORBANCE
1830 1820 1810 1800 1790 1780 1770 1760 1750 1740
FREQUENCY (cm^{-1})

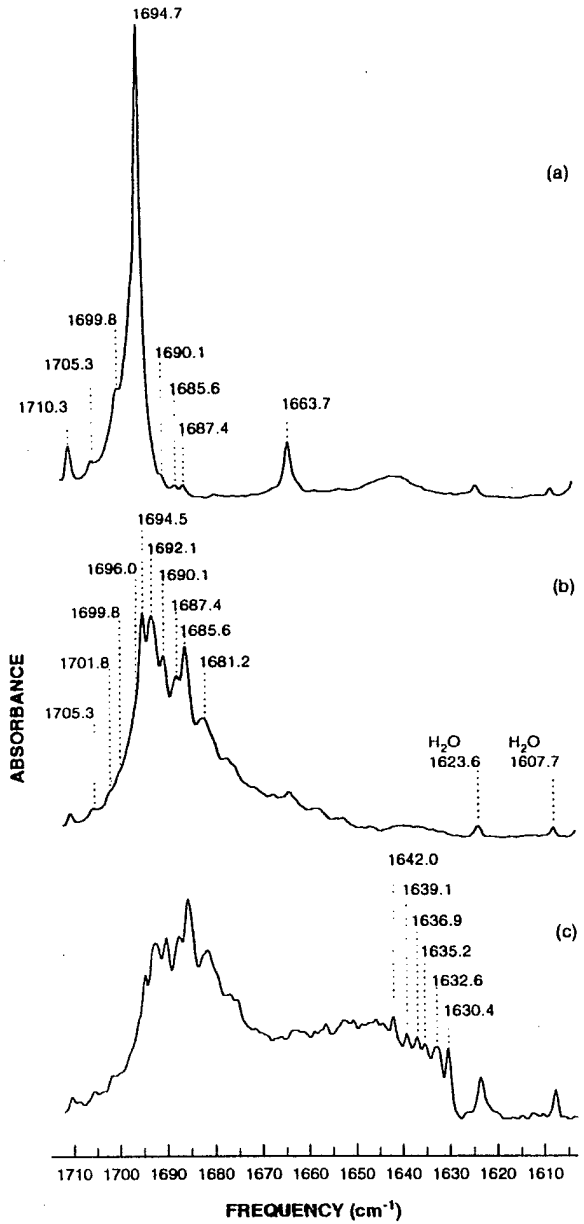
1694.7
(a)
1699.8
1705.3
1690.1
1685.6
1710.3
1687.4
1663.7
1694.5
1692.1
1696.0
1690.1
(b)
1687.4
1699.8
1685.6
1701.8
1681.2
1705.3
H_2O
1623.6
H_2O
1607.7
1642.0
1639.1
1636.9
(c)
1635.2
1632.6
1630.4
ABSORBANCE
1710 1700 1690 1680 1670 1660 1650 1640 1630 1620 1610
FREQUENCY (cm^{-1})

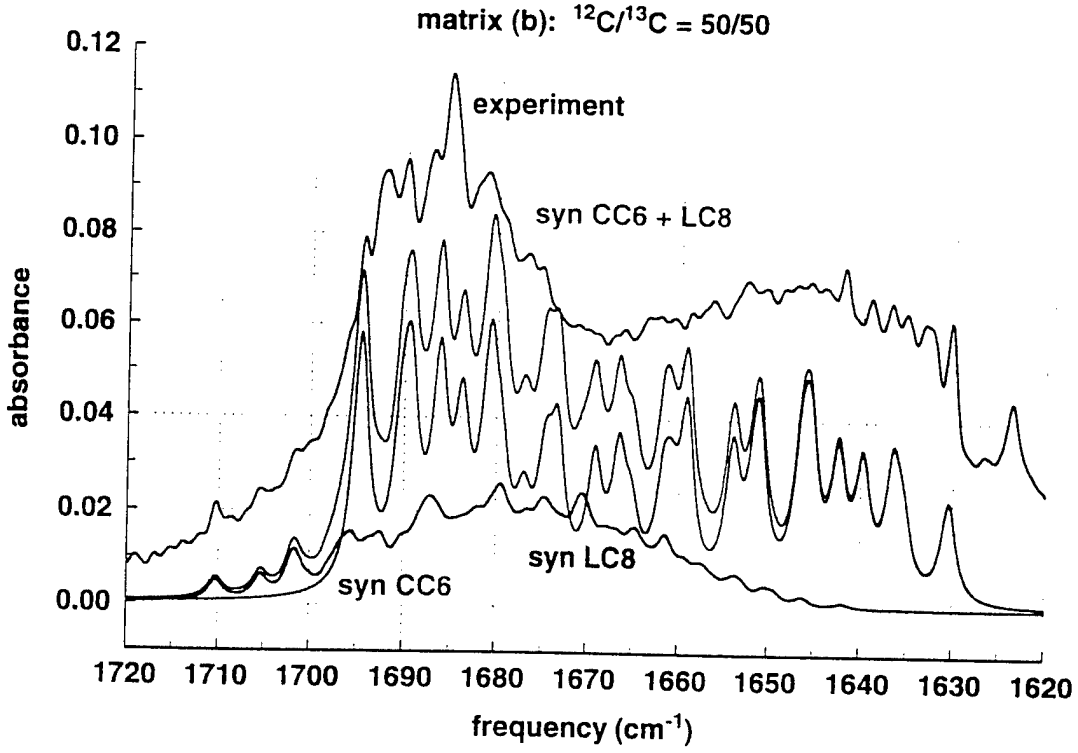
matrix (b): $^{12}C/^{13}C$ = 50/50
experiment
syn CC6 + LC8
syn LC8
syn CC6
absorbance
0.12
0.10
0.08
0.06
0.04
0.02
0.00
1720 1710 1700 1690 1680 1670 1660 1650 1640 1630 1620
frequency (cm^{-1})

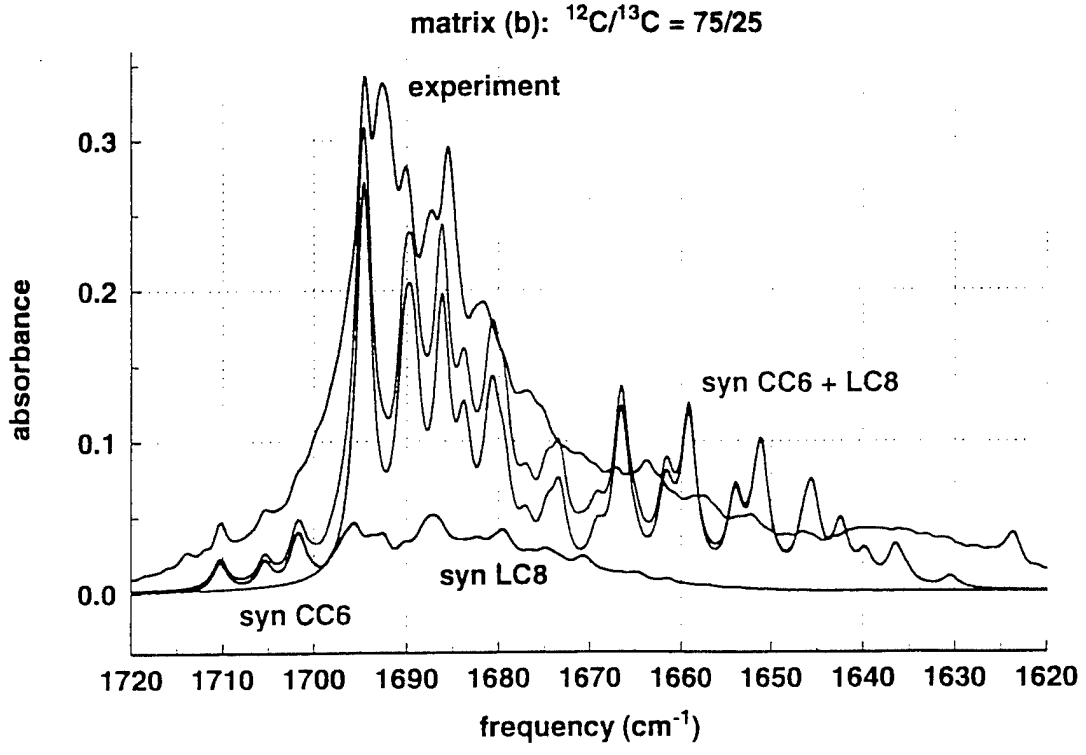
matrix (b): $^{12}C/^{13}C$ = 75/25
experiment
syn CC6 + LC8
syn LC8
syn CC6
absorbance
0.3
0.2
0.1
0.0
1720 1710 1700 1690 1680 1670 1660 1650 1640 1630 1620
frequency (cm^{-1})

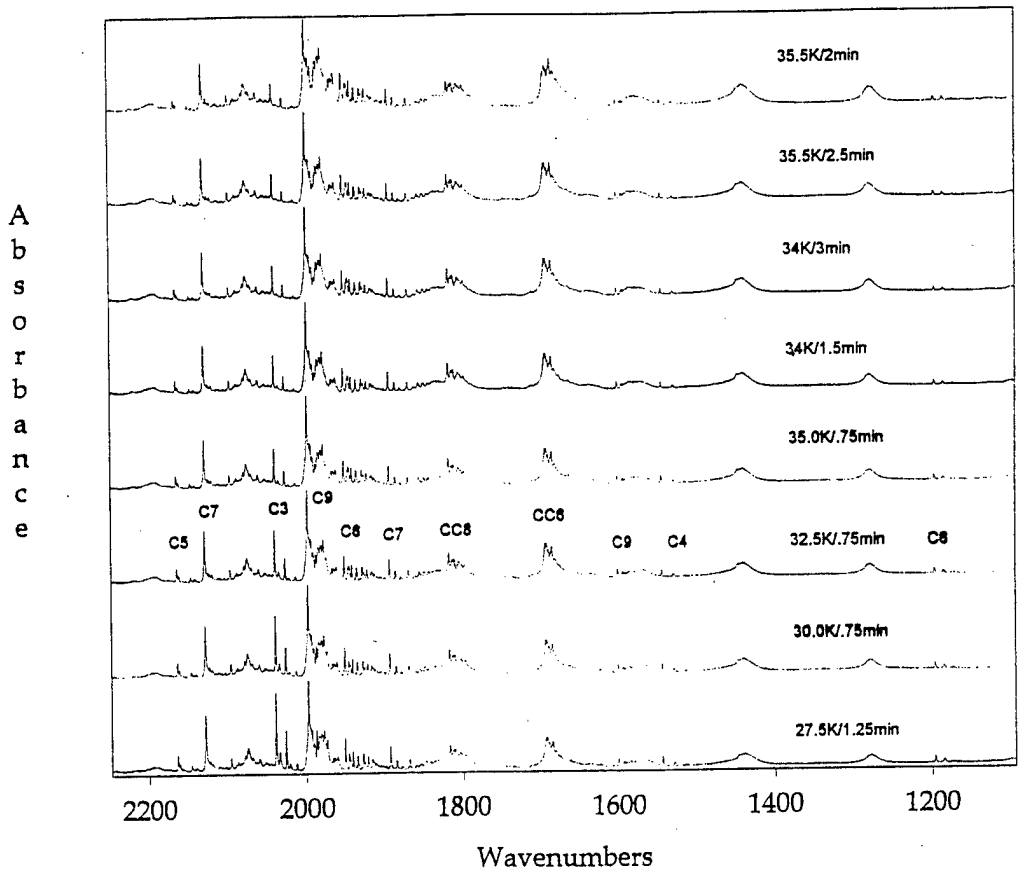
35.5K/2min
35.5K/2.5min
34K/3min
34K/1.5min
35.0K/.75min
32.5K/.75min
30.0K/.75min
27.5K/1.25min
C5
C7
C3
C9
C6
C7
CC6
CC6
C9
C4
C6
Absorbance
2200
2000
1800
1600
1400
1200
Wavenumbers

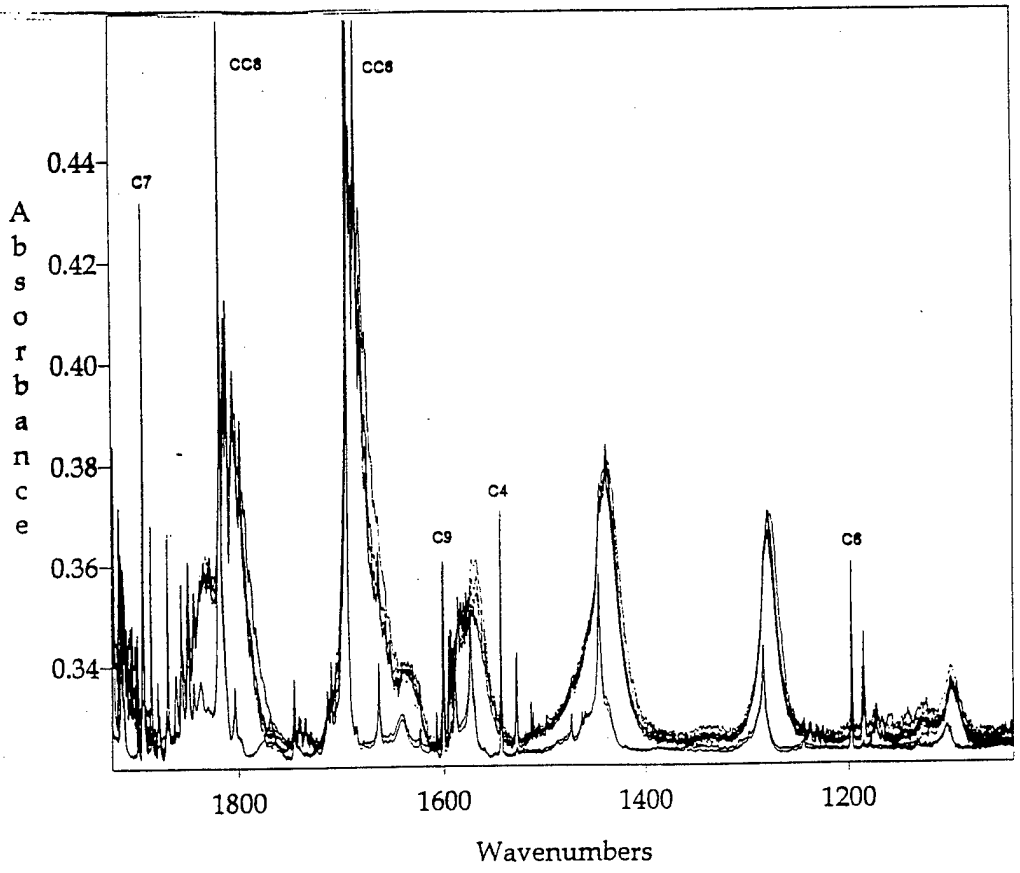
CC6
CC6
C7
C9
C4
C6
0.44
0.42
0.40
0.38
0.36
0.34
Absorbance
1800
1600
1400
1200
Wavenumbers

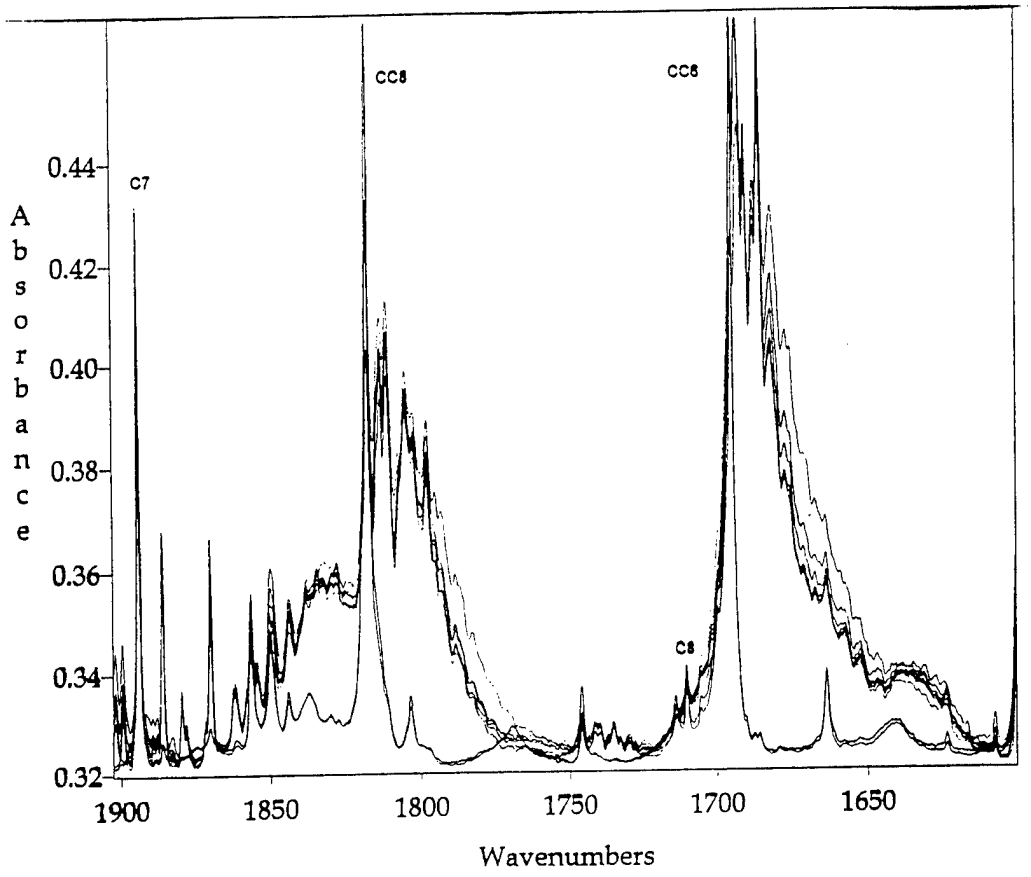
CC8
CC6
C7
C8
0.44
0.42
0.40
0.38
0.36
0.34
0.32
Absorbance
1900
1850
1800
1750
1700
1650
Wavenumbers

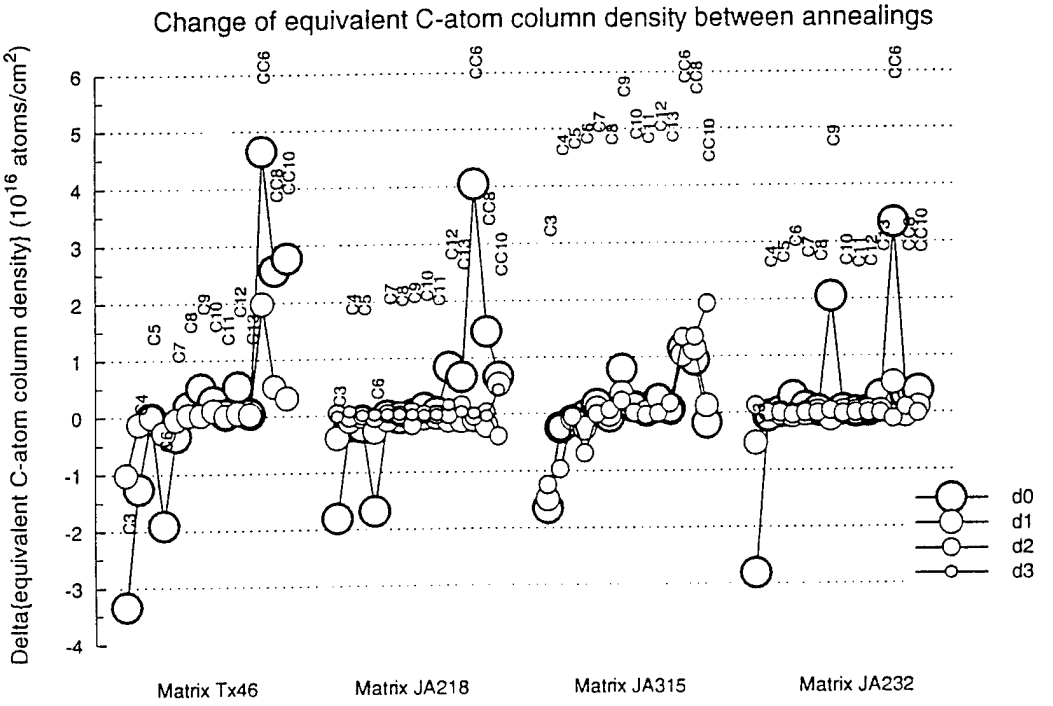
Change of equivalent C-atom column density between annealings
Delta{equivalent C-atom column density} (10^{16} atoms/cm^2)
6
5
4
3
2
1
0
-1
-2
-3
-4
d0
d1
d2
d3
Matrix Tx46
Matrix JA218
Matrix JA315
Matrix JA232
Ja218d7.axg May 7, 1998 4:34:33 PM

Comparison of C_4/C_6, C_7/C_9, C_{10}/C_{12} Ratios Obtained for Different Experimental Conditions

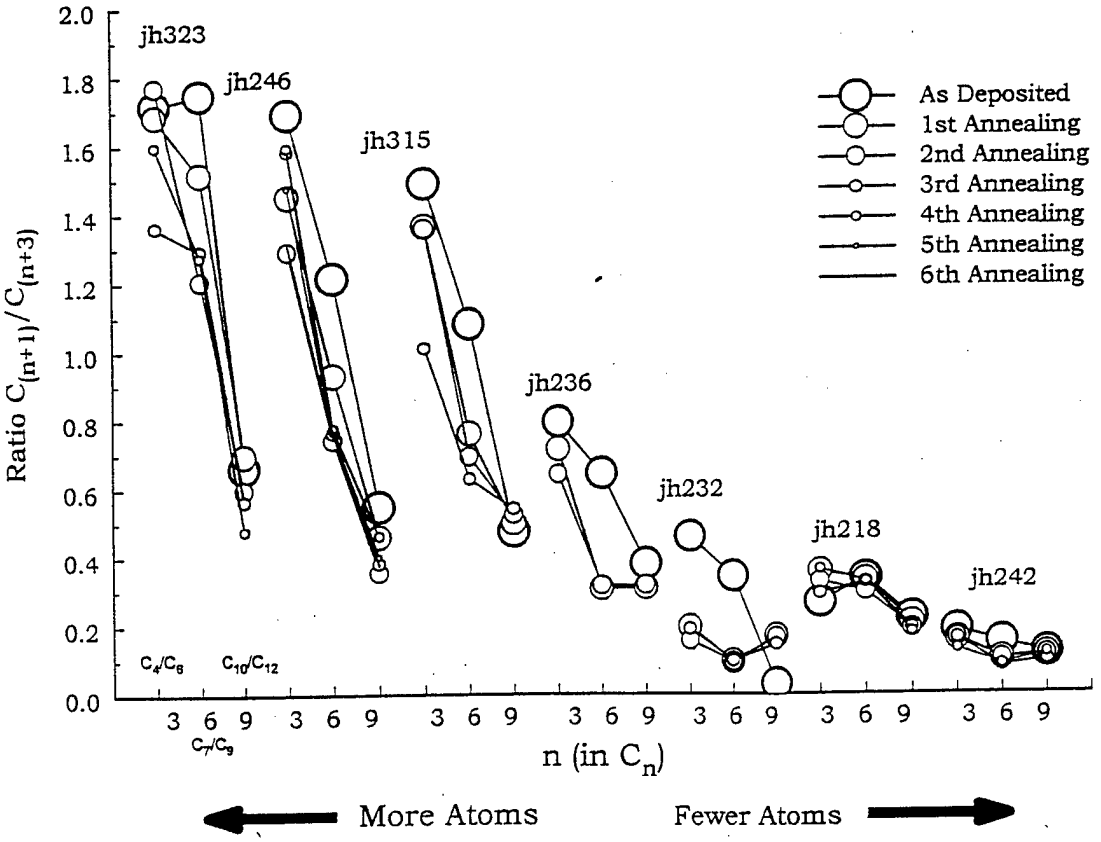

The ratio of the equivalent carbon atom column density for n+1 species (n as in C_n) to the equivalent carbon atom column density for n+3 species indicates how many atoms were available for formation of species like C_4, C_7, and C_{10}. When the Ta cell was hotter more n+1 species were formed during deposition than when the cell was colder. During annealings there were only minimal changes in the relative order of the ratios for C_4/C_6; C_7/C_9; C_{10}/C_{12}. Similar results are noted for C(n+2)/C(n+3).

The run with 5% H_2/95% Ar yields a lower C(n+1)/C(n+3) ratio than would be expected. The hydrogen may be scavenging atoms.

Comparison of C_5/C_6, C_8/C_9, C_{11}/C_{12} Ratios Obtained for Different Experimental Conditions

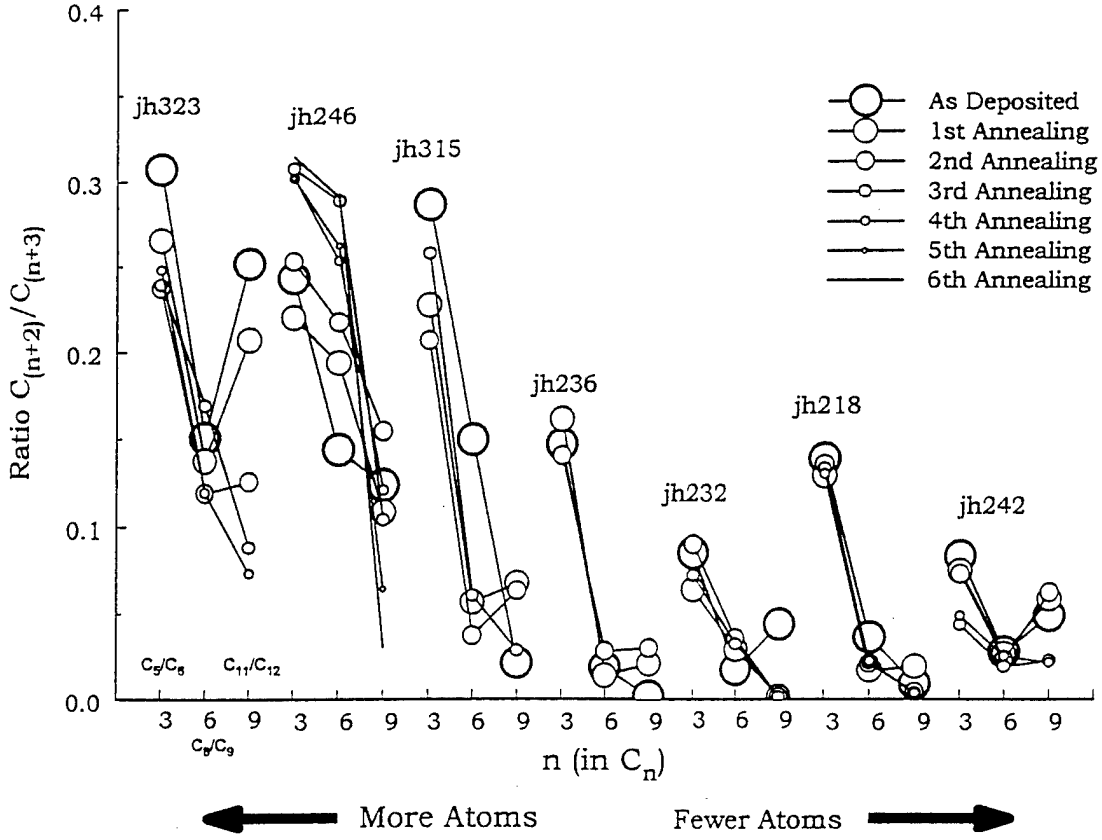

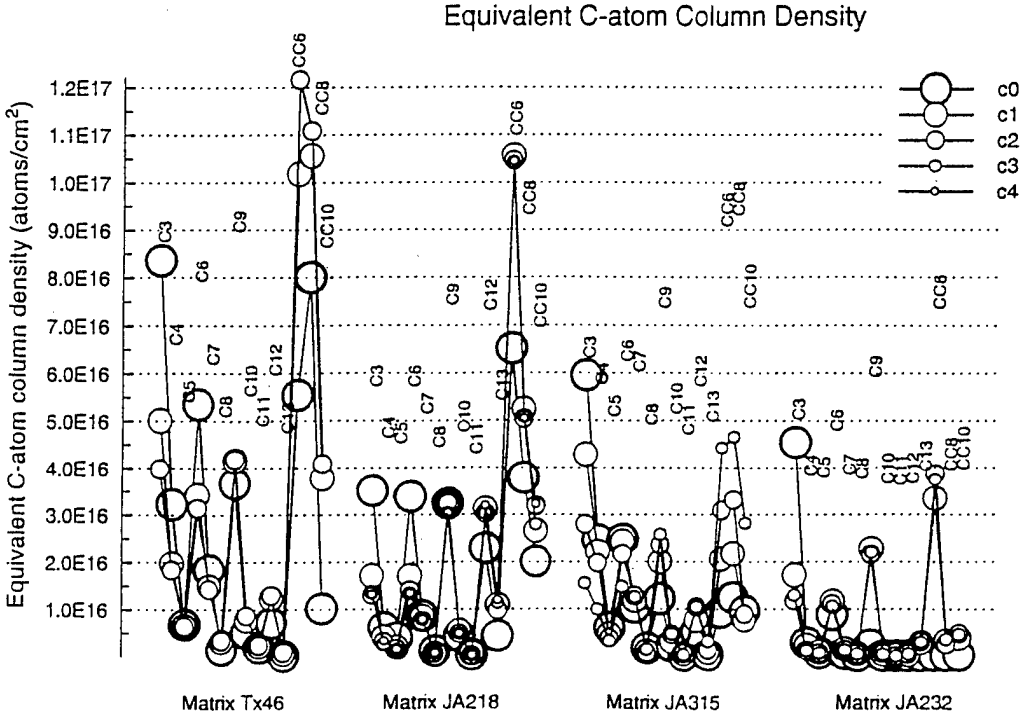

Cumulative Sum of Equivalent Carbon Atom Density

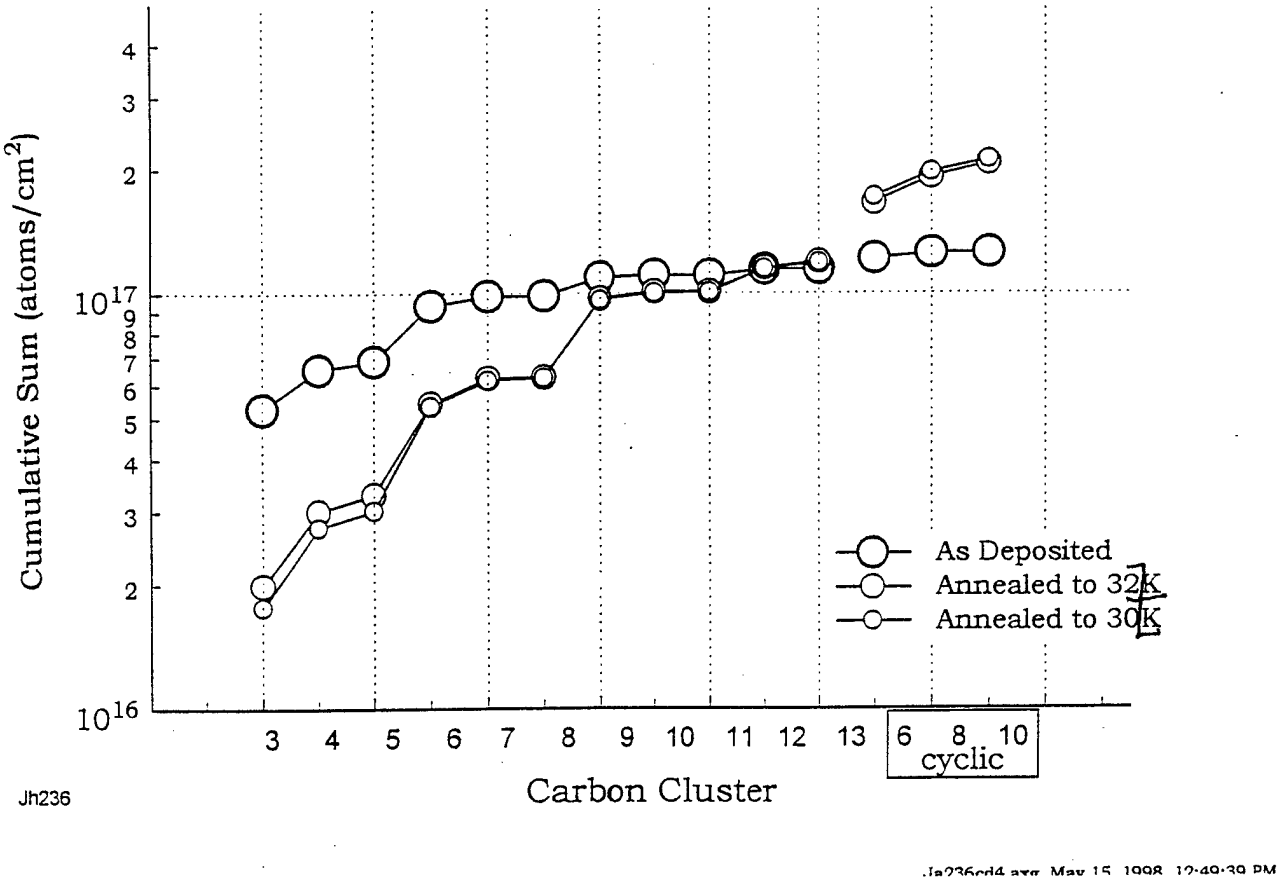

From successive cluster distributions one can calculate the quantity of carbon species that were not detected in the as-deposited matrix IR spectrum. This increase in the total equivalent carbon atom density is attributed to carbon atoms that are "invisible" to IR and were thus not accounted for in the original IR spectrum.

1= MixG+L (2053.7,.0078452,1.7666,.44691)
2= MixG+L (2051.9,.027381,1.4388,1.00E-06)
3= MixG+L (2050.3,.064283,1.434,.10607)
4= MixG+L (2048.9,.0052507,1.2237,.99803)
5= MixG+L (2047.9,.014253,1.9605,.99103)
6= Quadr (-.41118,.000086926,2.15E-09)

JLin

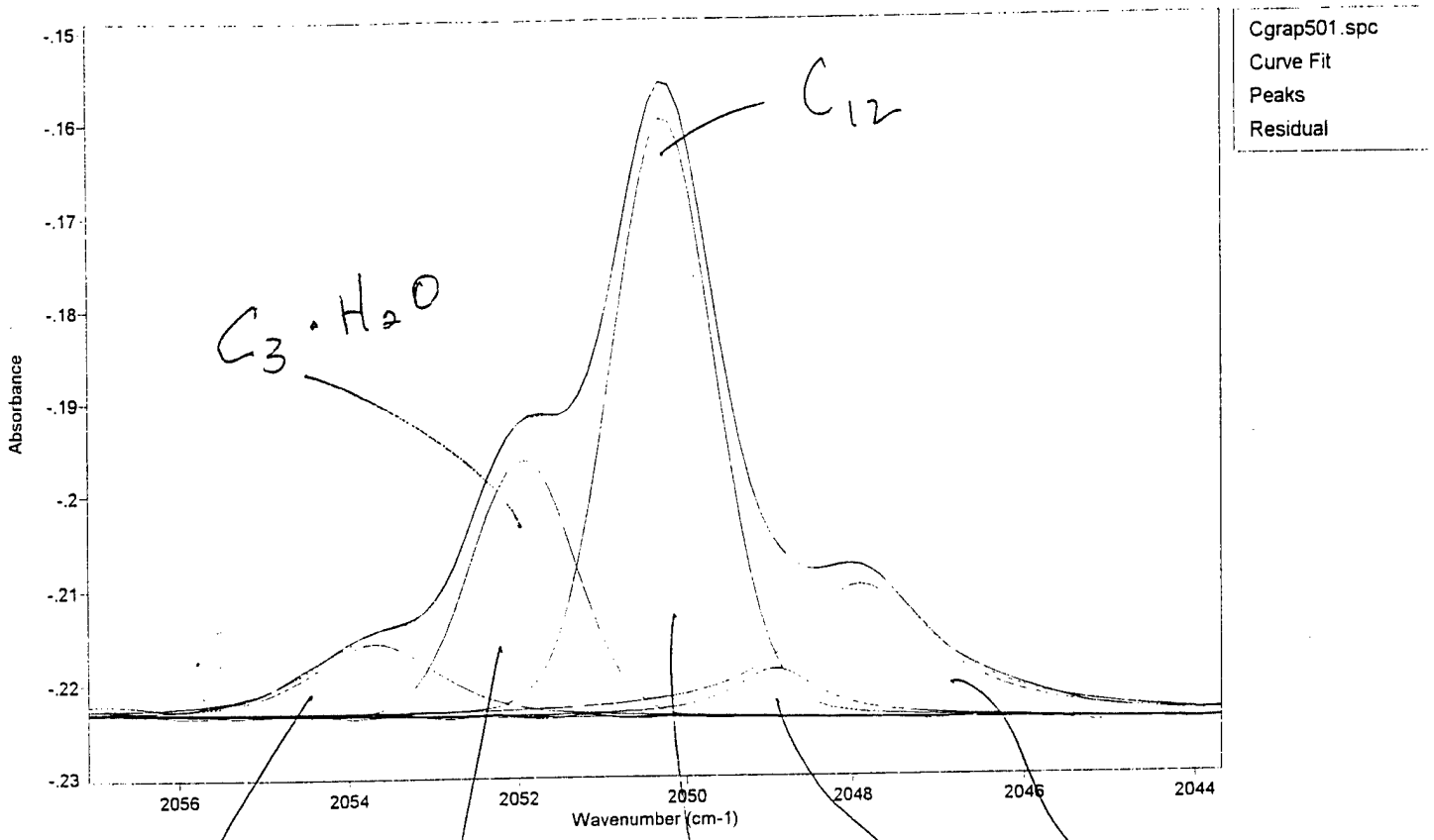

	2053.7	2051.9	2050.3	2048.9	2047.9
# =					5
Peak # →	1	2	3	4	
width →	1.7	1.4	1.4	1.2	1.9
% Concentration →	44%	0%	18%	99%	99%

Hanna Resler –

called w/ Wittig 4(3f)

JL

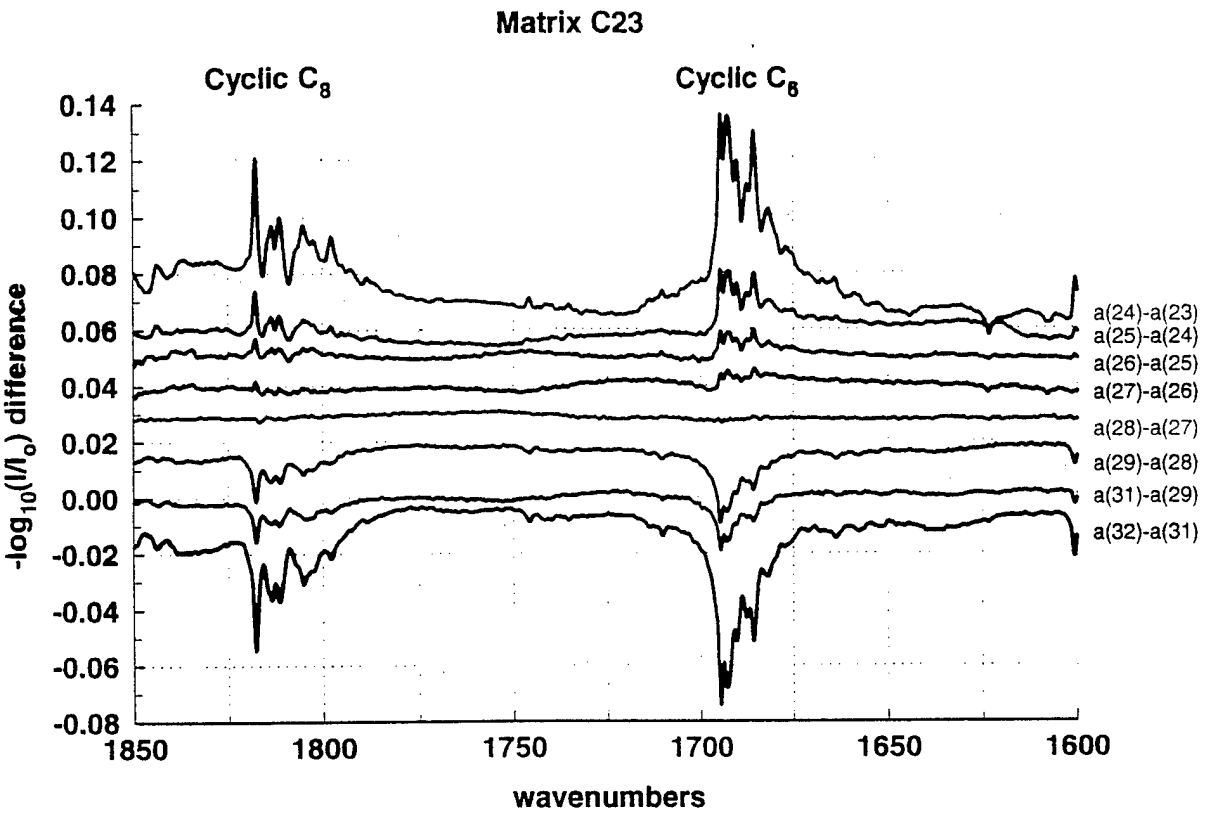

c6dif233.axg Phillips Lab, Edwards AFB, CA 93524 Sept. 11, 1997 3:15:09 PM

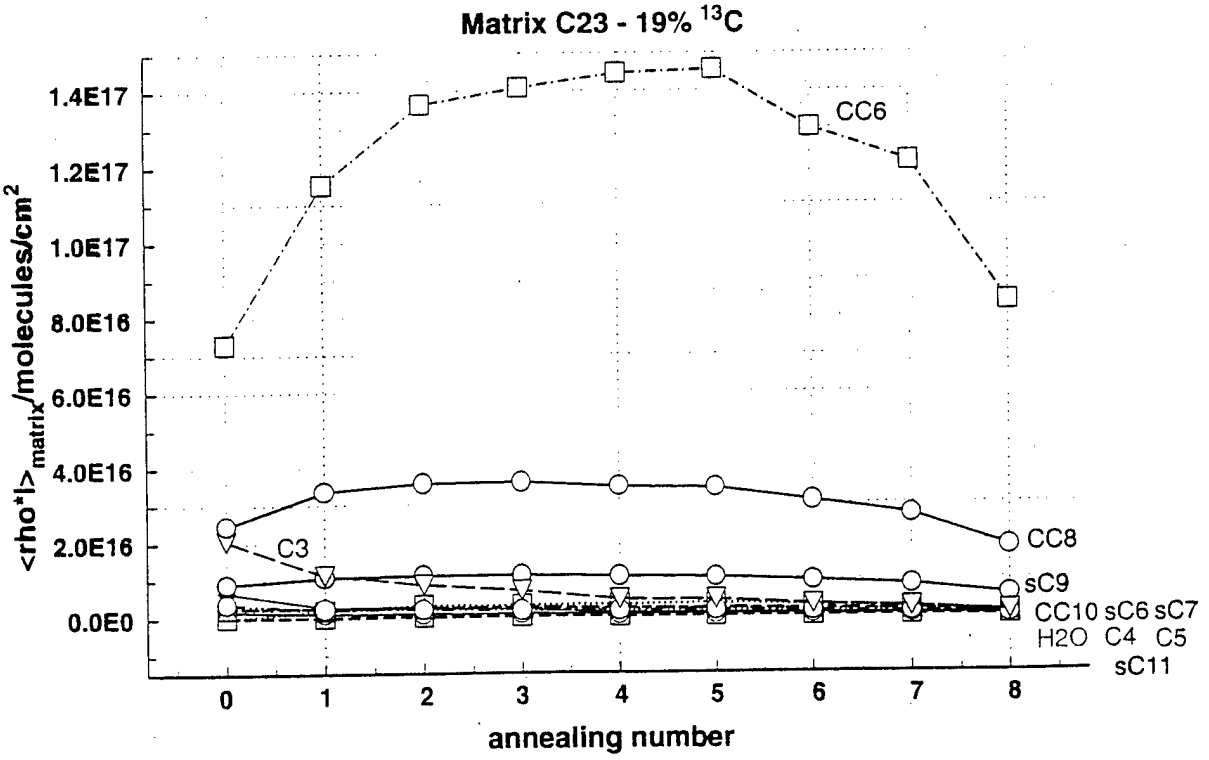

C23c2a.axg

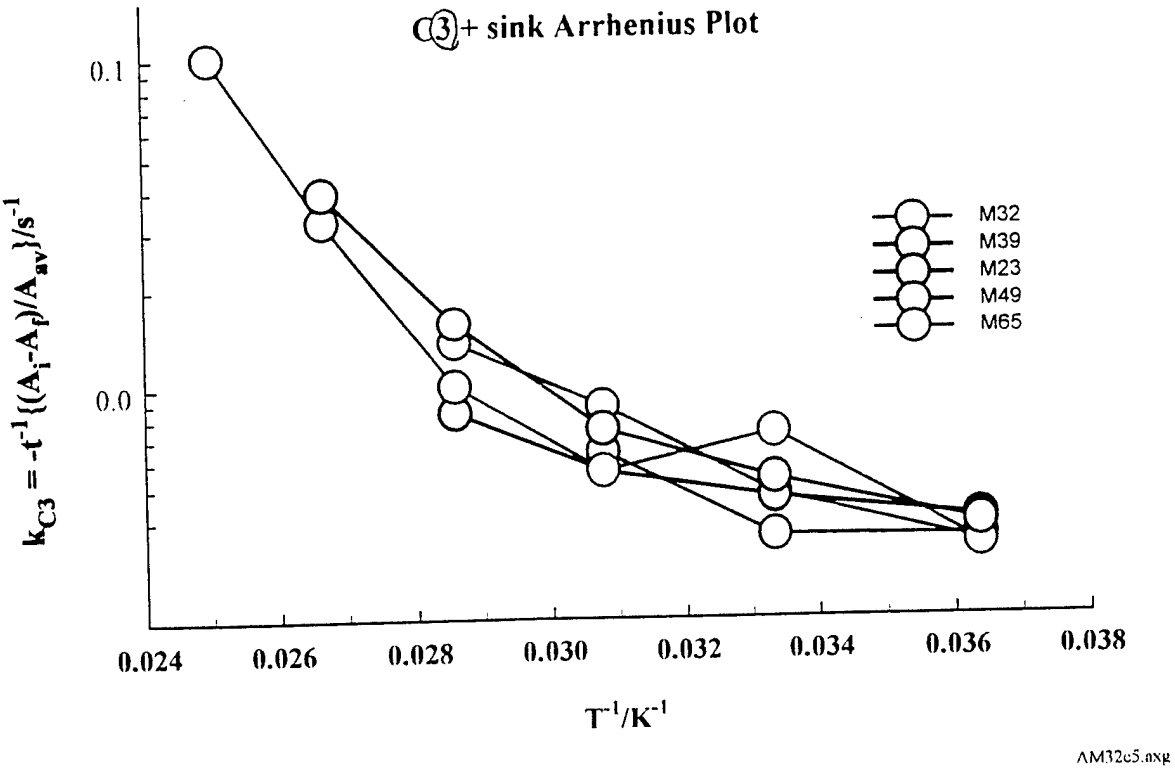
C3+ sink Arrhenius Plot
0.1
0.0
$k_{C3} = -t^{-1}\{(A_i-A_f)/A_{av}\}/s^{-1}$
M32
M39
M23
M49
M65
0.024
0.026
0.028
0.030
0.032
0.034
0.036
0.038
T^{-1}/K^{-1}
AM32c5.axg

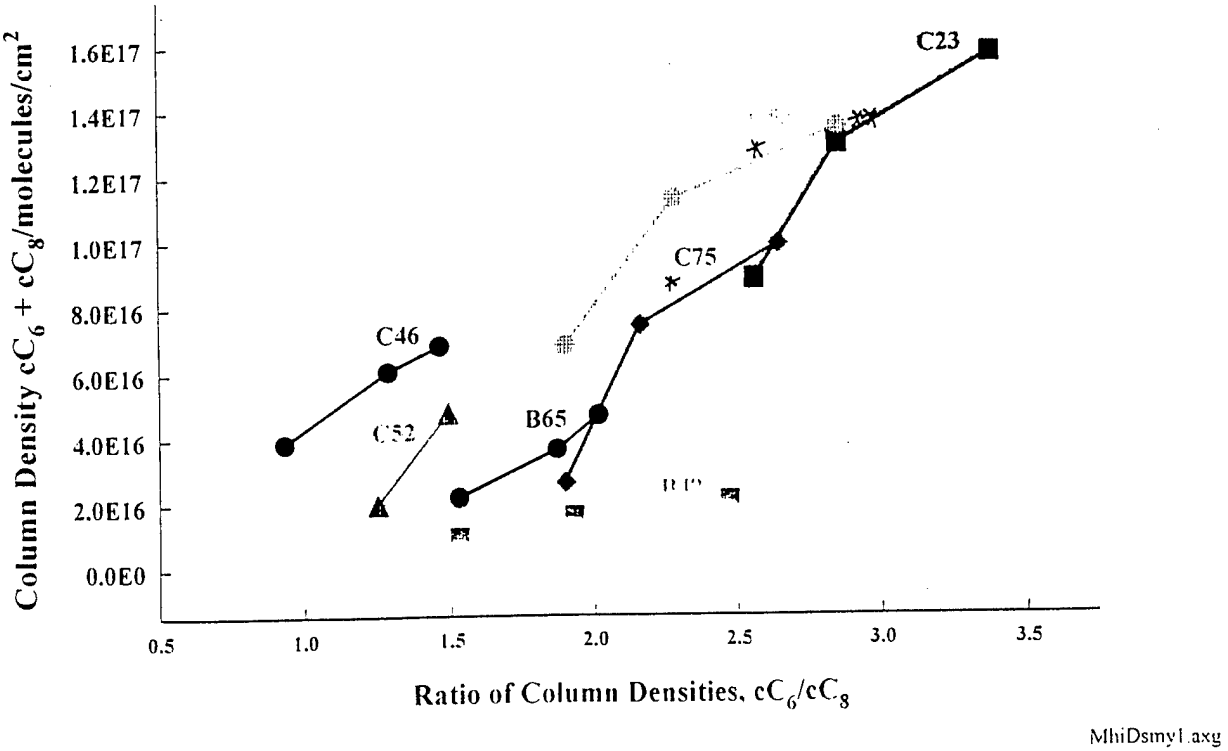
Cyclic C_6 and Cyclic C_8 in High Carbon Density Hedm Prototypes,
Column Density $cC_6 + cC_8$/molecules/cm^2
1.6E17
1.4E17
1.2E17
1.0E17
8.0E16
6.0E16
4.0E16
2.0E16
0.0E0
C23
C75
C46
C52
B65
0.5
1.0
1.5
2.0
2.5
3.0
3.5
Ratio of Column Densities, cC_6/cC_8
MhiDsmy1.axg

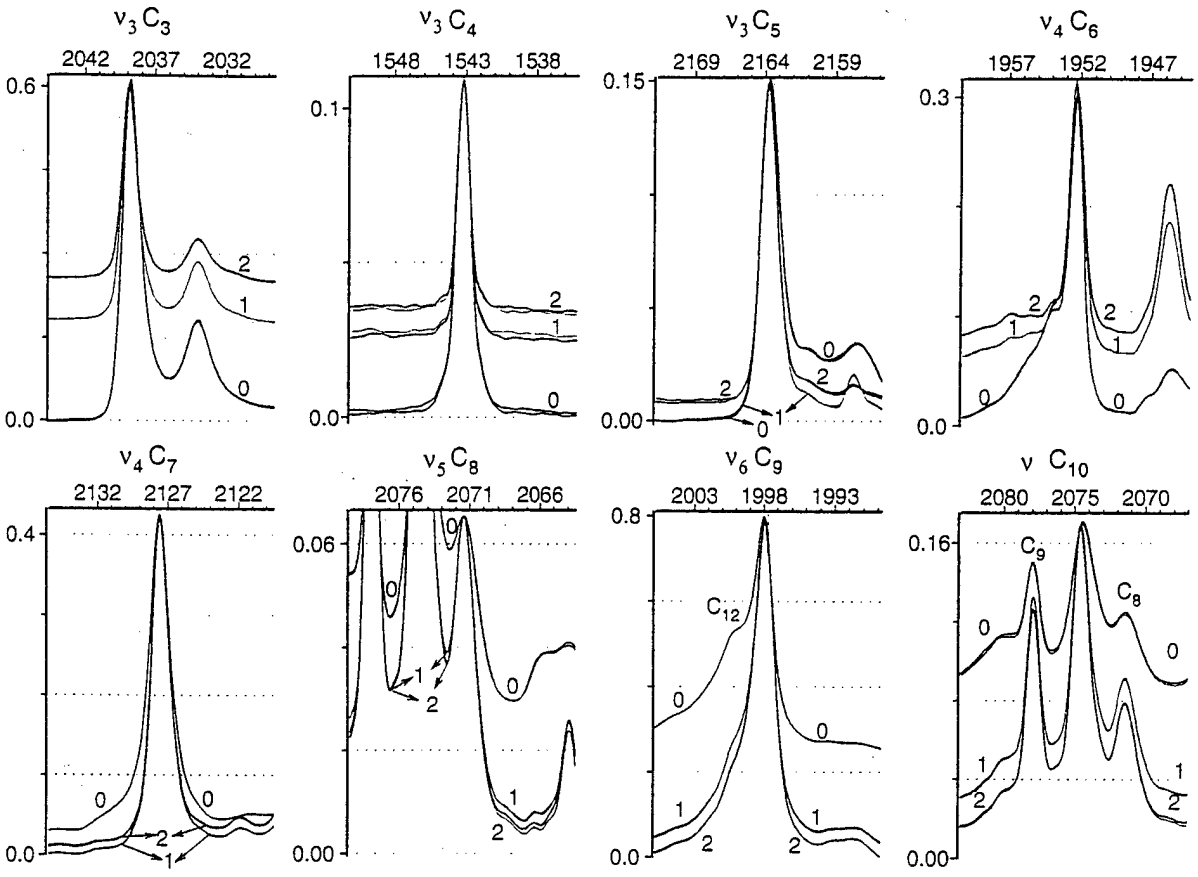

Carbon Matrix (a) - C_n Clusters

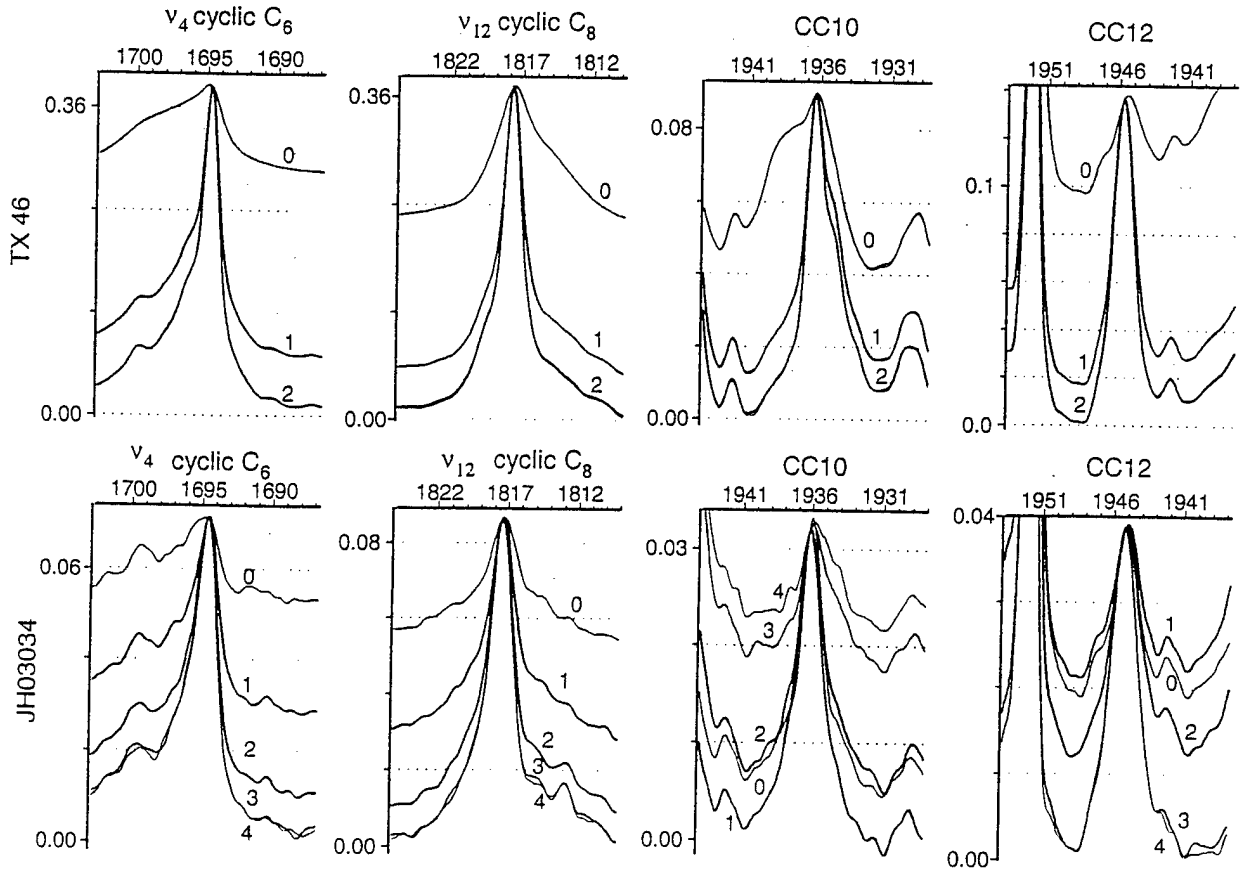

Carbon Matrix Tx 46 JA03034

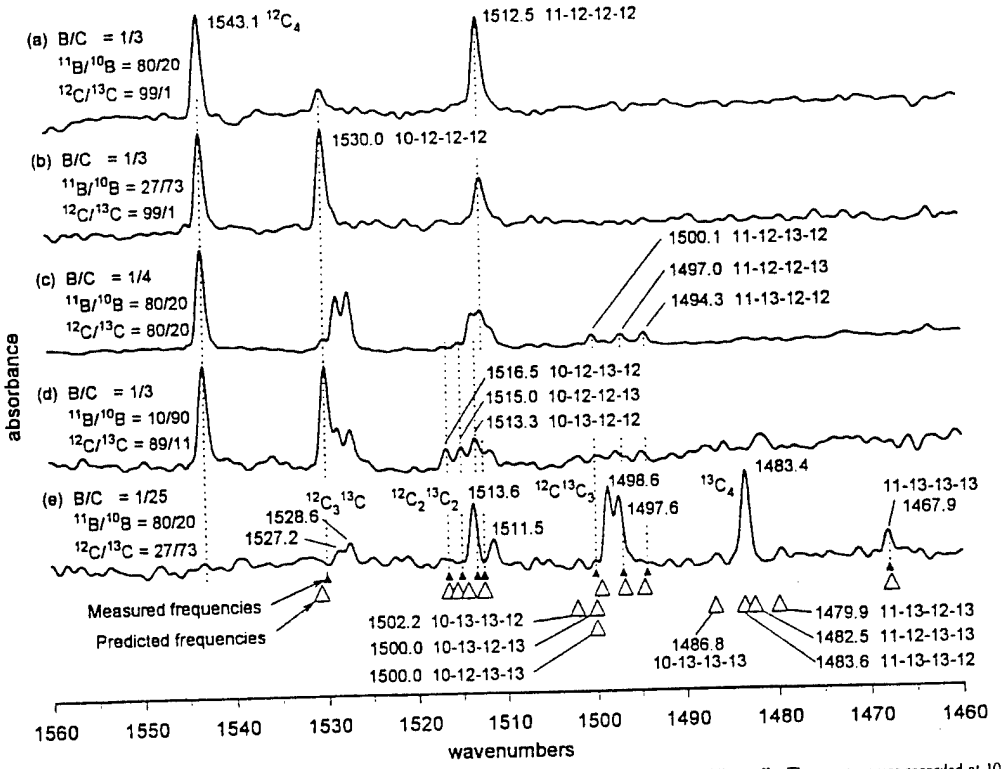

FIG. 1. FTIR spectra of the $\nu_2(\sigma)$ mode of isotopomers of linear BC_3 and the $\nu_3(\sigma_u)$ mode of isotopomers of linear C_4. The spectra were recorded at 10 K after annealing the matrices with the indicated compositions at 27.5 K for 150 s. The large open triangles at the bottom show the predicted frequencies of linear BC_3 isotopomers (as explained in the text) and small filled triangles show measured isotopomer frequencies.

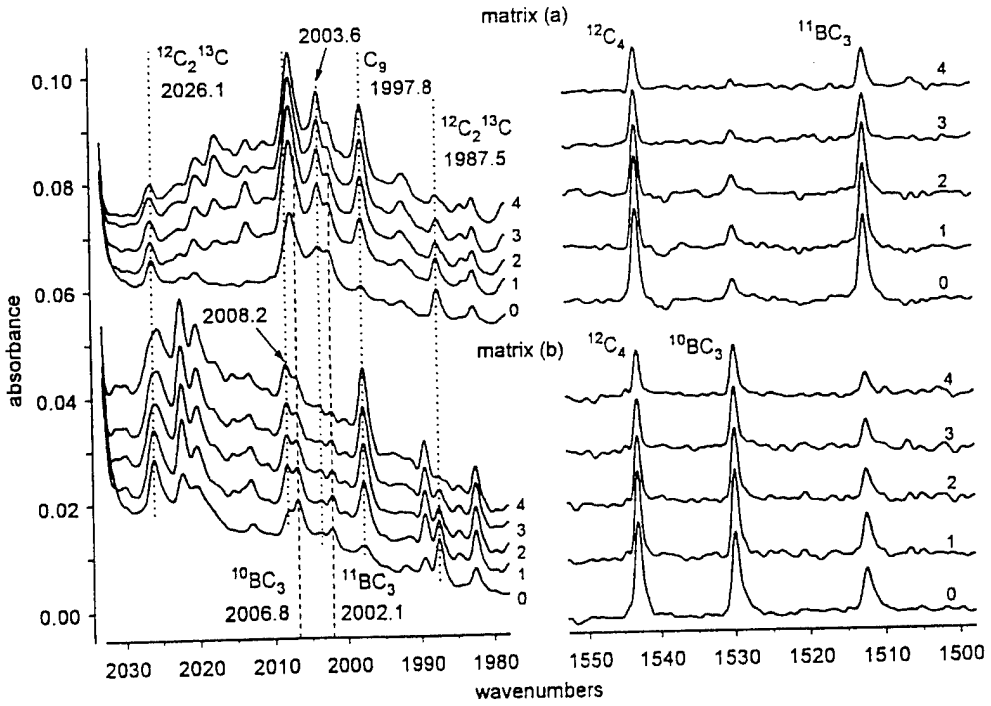

FIG. 2. Spectra obtained from matrix (a) [$^{11}B/^{10}B = 4/1$] and matrix (b) [$^{11}B/^{10}B = 1/2.7$] showing correlation upon annealing of the $\nu_1(\sigma)$ bands of $^{10}BC_3$ and $^{11}BC_3$ at 2006.8 and 2002.1 cm^{-1} with the $\nu_2(\sigma)$ bands at 1530.0 and 1512.5 cm^{-1}. The spectra labeled "0" are from the originally deposited matrix. Labels "1" to "4" indicate spectra recorded after the first through fourth annealing as follows: (1) 27.5 K for 150 s, (2) 30.0 K for 75 s, (3) 32.5 K for 45 s, (4) 35.0 K for 30 s. Frequency and absorbance scales are identical for all spectra. The plotted absorbance is $-\log_{10}$ of the transmittance. To facilitate comparisons between matrices, the absorbance of the matrix (b) spectra are multiplied by 1.4.

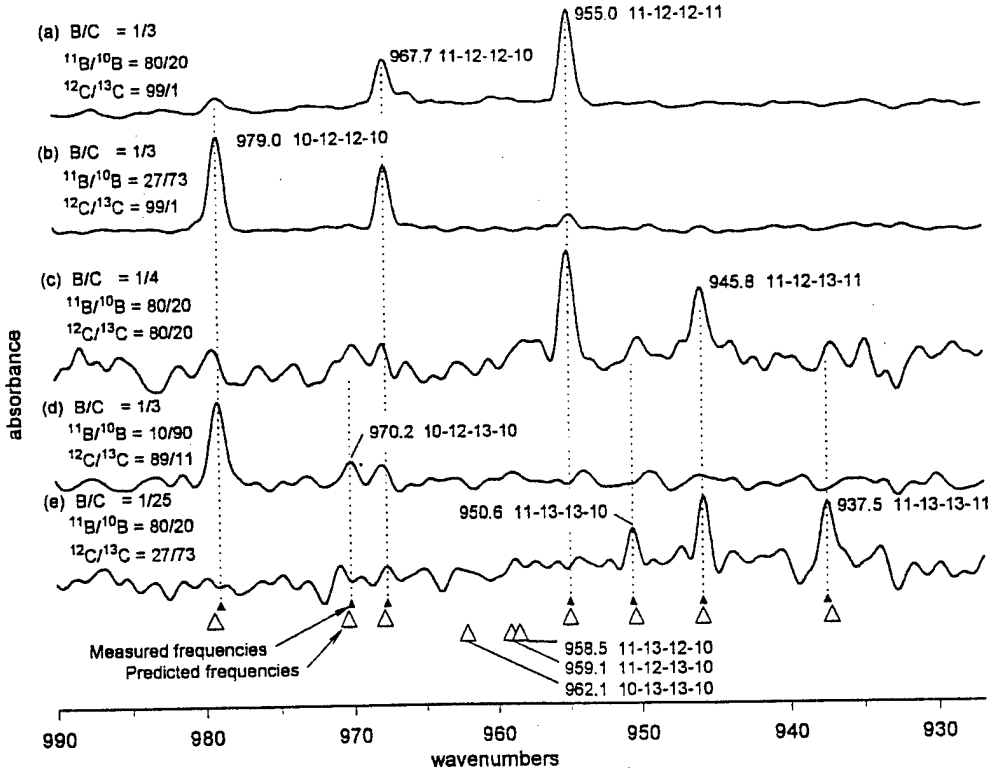

FIG. 3. FTIR spectra of the $\nu_3(\sigma_u)$ mode of isotopomers of linear BCCB. The spectra were recorded after annealing the matrices with the indicated compositions at 27.5 K for 150 s. The large open triangles at the bottom show the predicted frequencies of linear BCCB isotopomers (as explained in the text) and small filled triangles show measured isotopomer frequencies.

TABLE IV. Experimental B_2C_2 isotopomer frequency patterns. Frequencies and frequency intervals (cm^{-1}) in triplet bands of B_2C_2 isotopomers.

Boron isotope triplets				Carbon isotope triplets			
		Intervals				Intervals	
Isotopomer	Freq.	Short	Long	Isotopomer	Freq.	Short	Long
$^{10}B_2\,^{12}C_2$	979.0			$^{10}B_2\,^{12}C_2$	979.0		
		11.3				8.8	
$^{10,11}B_2\,^{12}C_2$	967.7		24.0	$^{10}B_2\,^{12,13}C_2$	970.2		(16.7)[a]
		12.7				(7.9)[a]	
$^{11}B_2\,^{12}C_2$	955.0			$^{10}B_2\,^{13}C_2$	(962.3)[a]		
$^{10}B_2\,^{12,13}C_2$	970.2			$^{10,11}B_2\,^{12}C_2$	967.7		
		(11.5)[a]				(9.0)[a]	
$^{10,11}B_2\,^{12,13}C_2$	(958.7)[a]		24.4	$^{10,11}B_2\,^{12,13}C_2$	(958.7)[a]		17.1
		(12.9)[a]				(8.1)[a]	
$^{11}B_2\,^{12,13}C_2$	945.8			$^{10,11}B_2\,^{13}C_2$	950.6		
$^{10}B_2\,^{13}C_2$	(962.3)[a]			$^{11}B_2\,^{12}C_2$	955.0		
		(11.7)[a]				9.2	
$^{10,11}B_2\,^{13}C_2$	950.6		(24.8)[a]	$^{11}B_2\,^{12,13}C_2$	945.8		17.5
		13.1				8.3	
$^{11}B_2\,^{13}C_2$	937.5			$^{11}B_2\,^{13}C_2$	937.5		

[a]Frequencies and intervals in parentheses were interpolated or extrapolated from measured quantities.

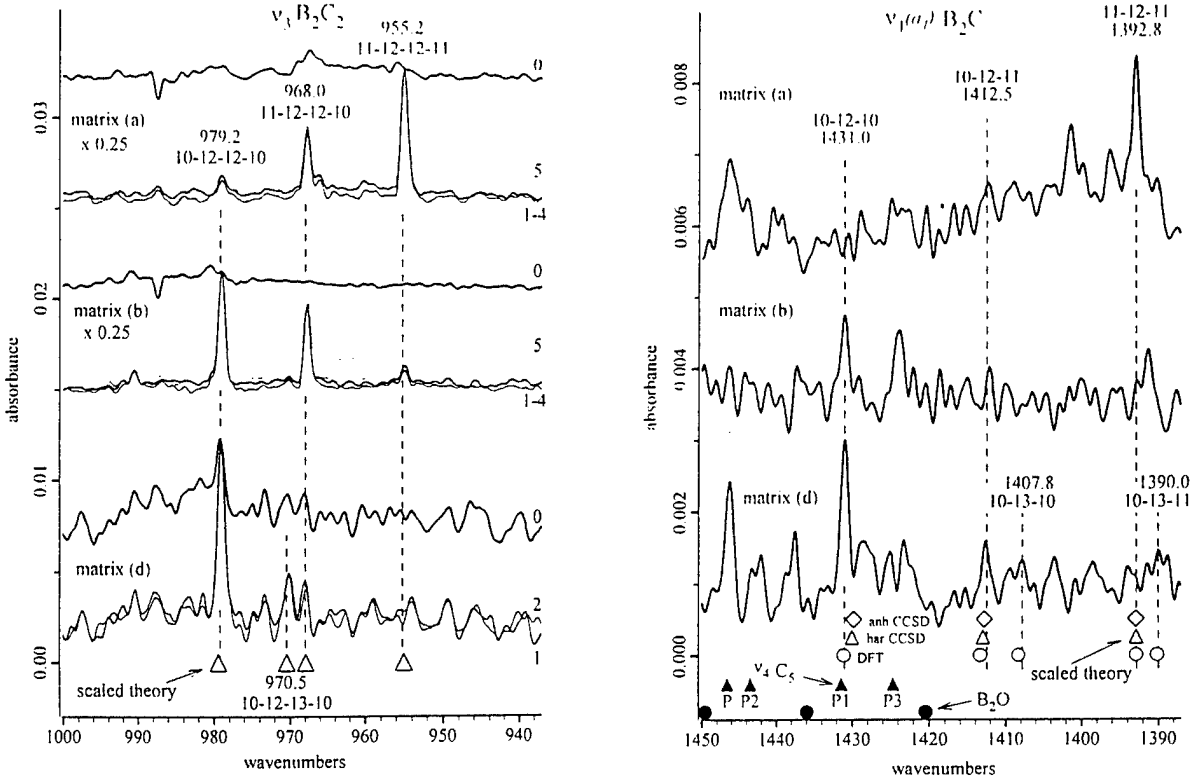

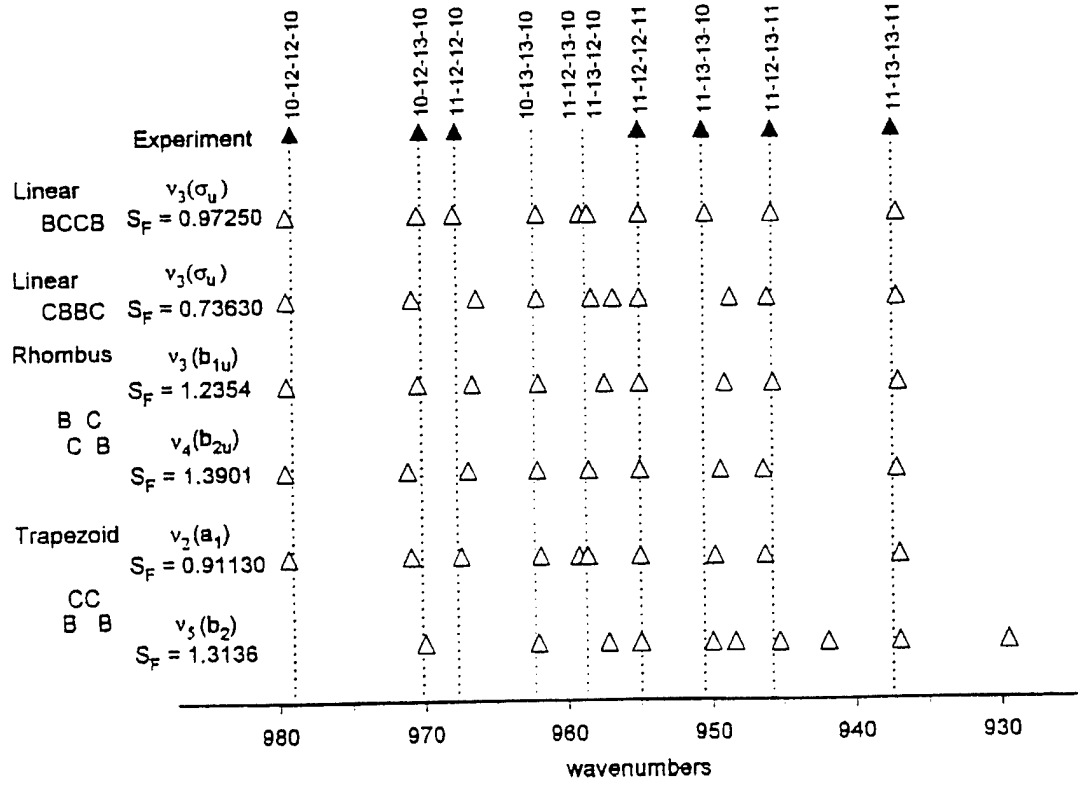

FIG. 4. Comparison of experimental isotopomer frequencies to scaled theoretical isotopomer frequencies for the most intense modes of four B_2C_2 geometries as calculated by Rittby, Ref. 5.

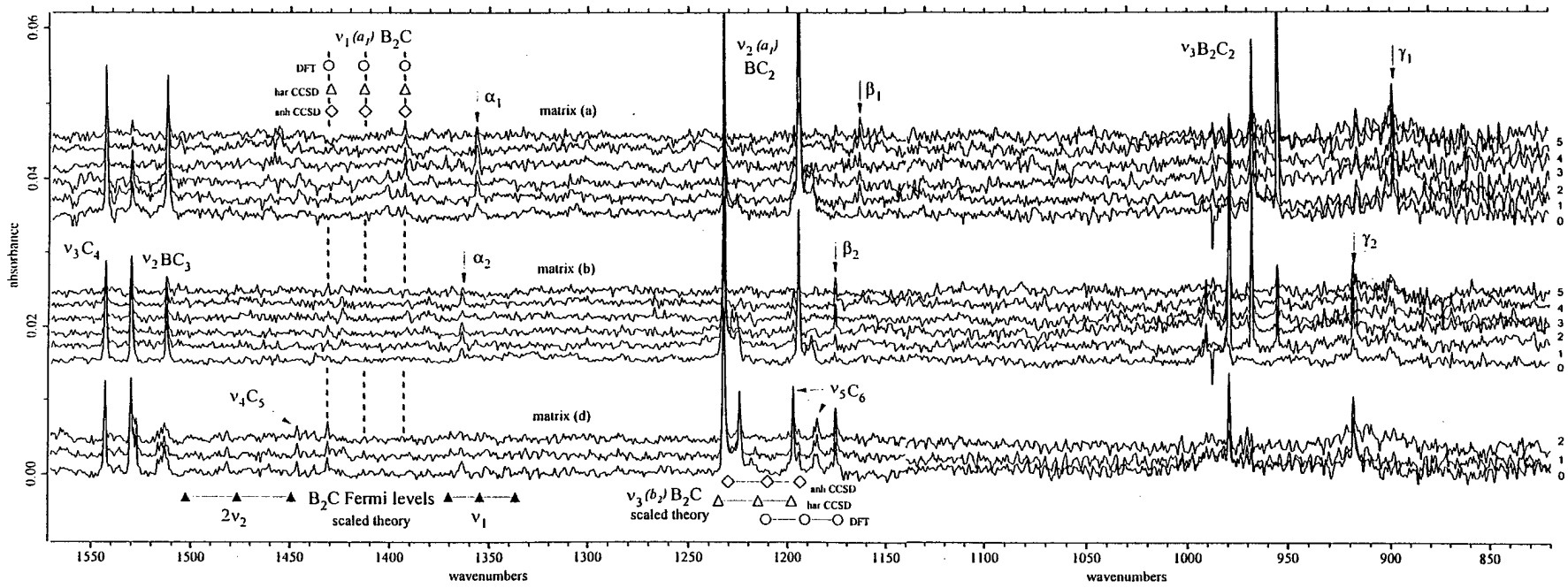
absorbance
0.06
0.04
0.02
0.00
$\nu_1(a_1)$ B_2C
DFT
har CCSD
anh CCSD
α_1
matrix (a)
$\nu_2(a_1)$
BC_2
β_1
$\nu_3B_2C_2$
γ_1
ν_3C_4
ν_2BC_3
α_2
matrix (b)
β_2
γ_2
ν_4C_5
matrix (d)
ν_5C_6
B_2C Fermi levels
$2\nu_2$
scaled theory
ν_1
$\nu_3(b_2)$ B_2C
scaled theory
anh CCSD
har CCSD
DFT
1550
1500
1450
1400
1350
1300
1250
1200
1150
1100
1050
1000
950
900
850
wavenumbers
wavenumbers

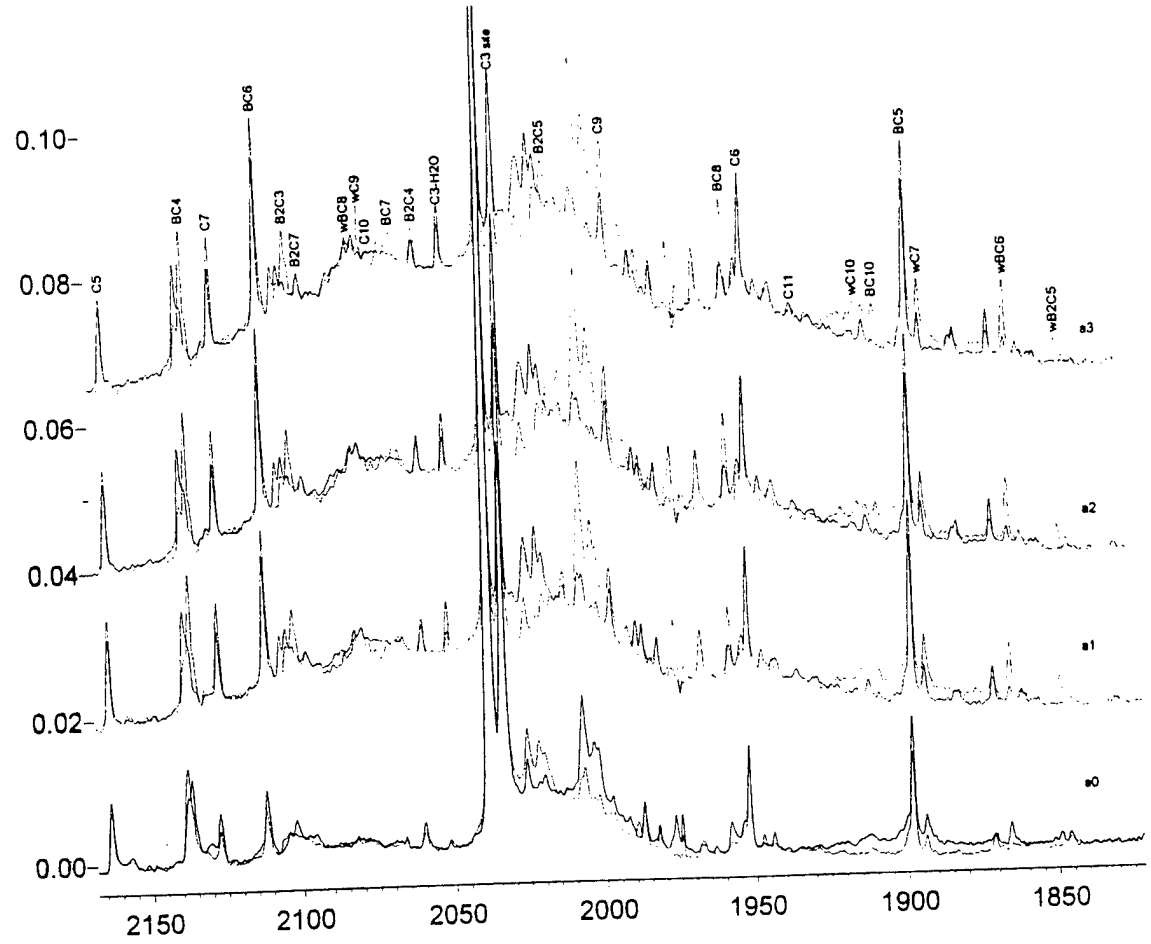
0.10
0.08
0.06
0.04
0.02
0.00
C5
BC4
C7
BC6
B2C3
B2C7
wBC8
wC9
C10
BC7
B2C4
C3-H2O
C3
B2C5
C9
BC8
C6
C11
wC10
BC10
BC5
wC7
wBC6
wB2C5
s3
s2
s1
s0
2150
2100
2050
2000
1950
1900
1850

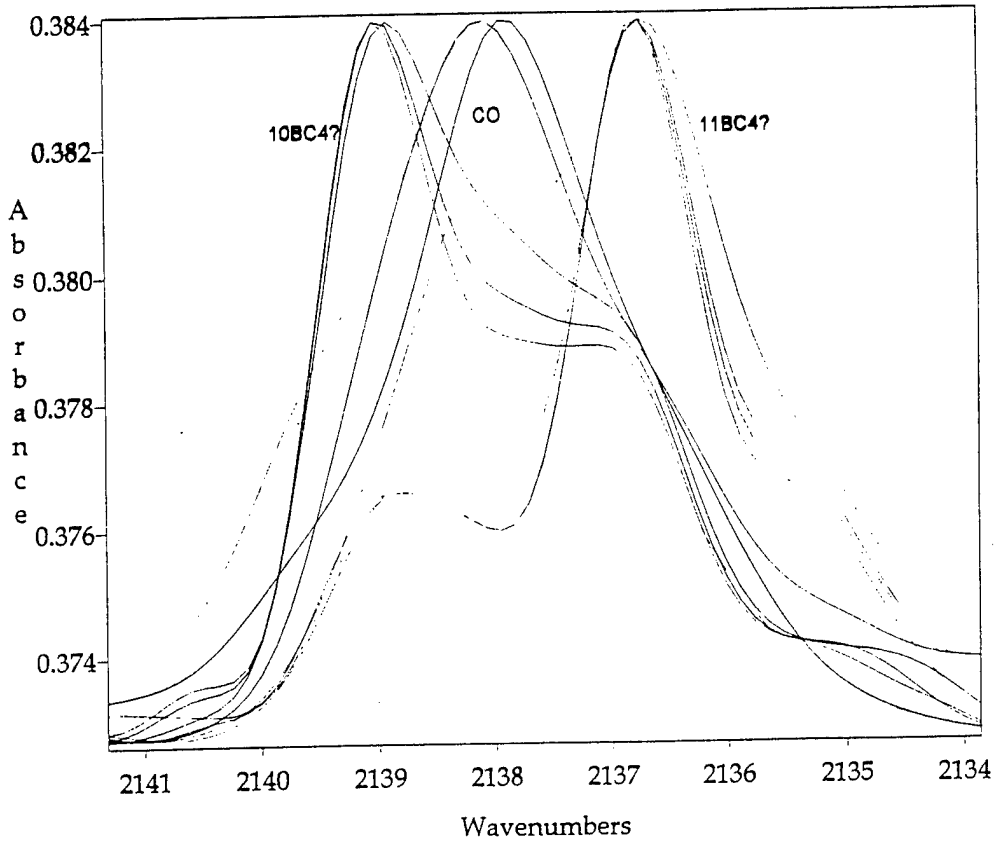
0.384
0.382
0.380
0.378
0.376
0.374
Absorbance
10BC4?
CO
11BC4?
2141
2140
2139
2138
2137
2136
2135
2134
Wavenumbers

B/C@1898.4
0.390
0.385
0.380
Absorbance
1900
1899
1898
1897
Wavenumbers

?

B/C @ 2112.0
0.384
0.383
0.382
0.381
0.380
0.379
0.378
Absorbance
2113.5
2113.0
2112.5
2112.0
2111.5
2111.0
2110.5
Wavenumbers

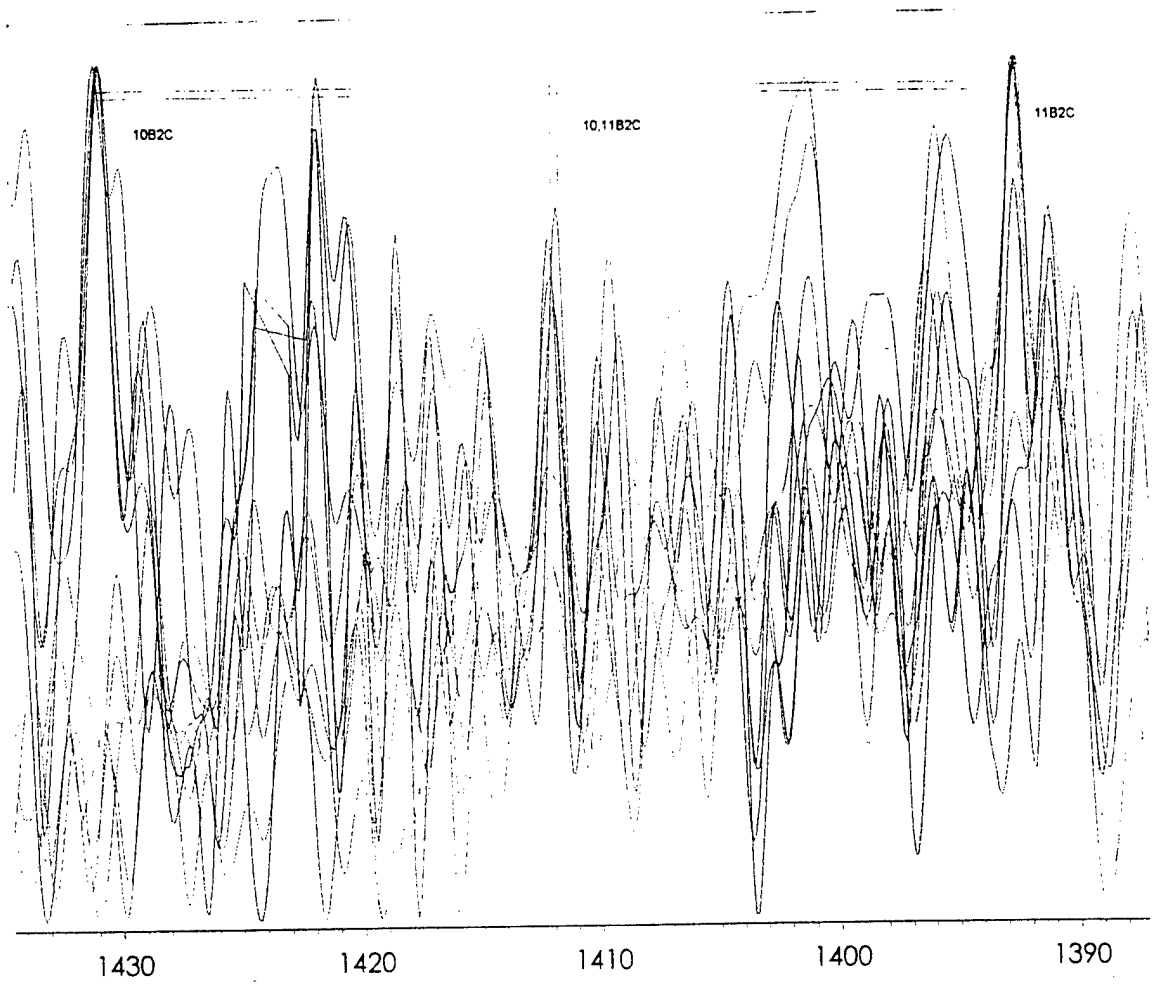
10B2C
10,11B2C
11B2C
1430
1420
1410
1400
1390

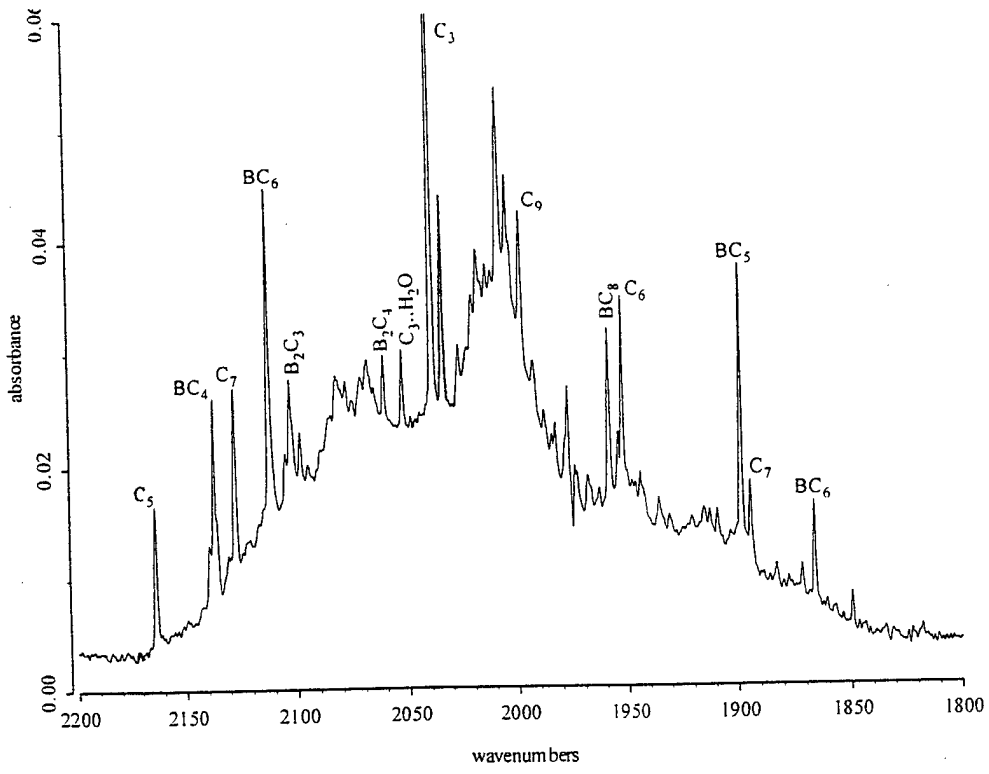

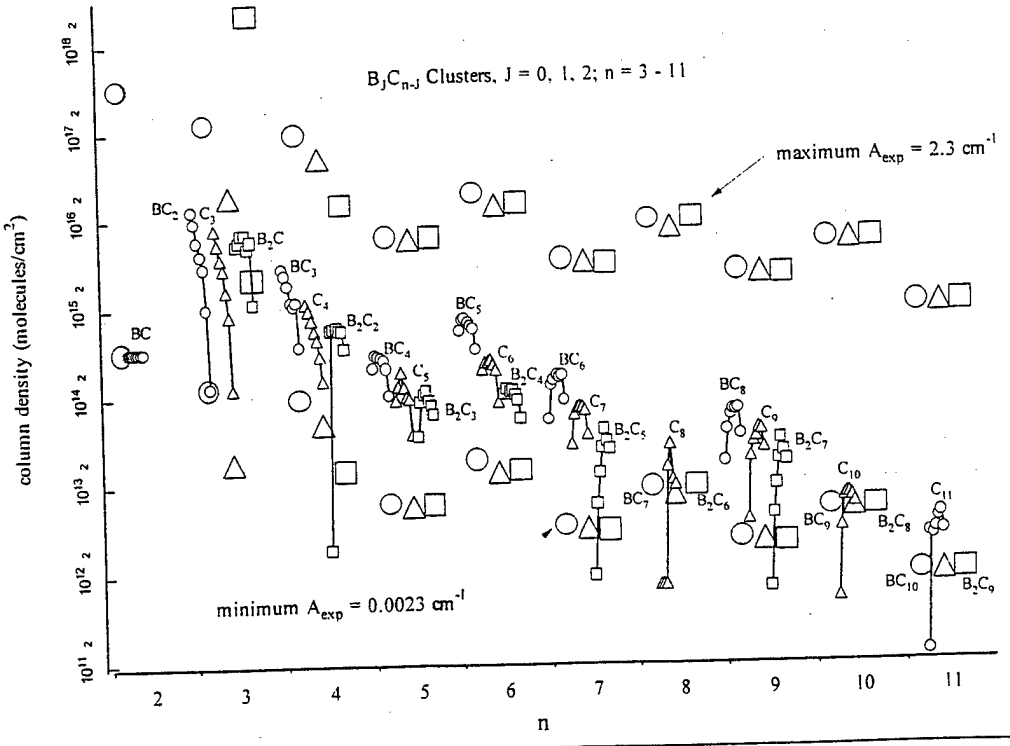

Figure 1. Distribution of B_JC_{n-J} clusters. J = 0, 1, 2; n = 3 - 11. Circles, triangles and squares represent BC_{n-1}, C_n, and BC_{n-2} clusters, respectively. Large symbols denote upper and lower limits of measurement, based on a nominal minimum measurable absorbance of 0.0023 cm^{-1}, and a maximum absorbance for linearity of Beer's law of 2.3 cm^{-1} (1% transmittance. Small symbols denote measured quantities in the initial matrix, and in six annealed matrices. Annealing temperatures and times were (1) 27.5 K/150 s, (2) 30.0 K/75 s, (3) 32.5 K/45 s, (4) 35.0 K/30 s, (5) 37.5 K/20 s, (6) 40.0 K/20 s. The decreases in column density in the fifth and sixth annealing are due to matrix sublimation. Some of the larger clusters (n = 8, 10, 11) have not been identified, BC_7, B_2C_6, BC_9, B_2C_8, BC_{10}, B_2C_9.

J = 0 1 2

matrix (a): $^{11}B/^{10}B$ = 80/20, $^{12}C/^{13}C$ = 99/1

n = 3

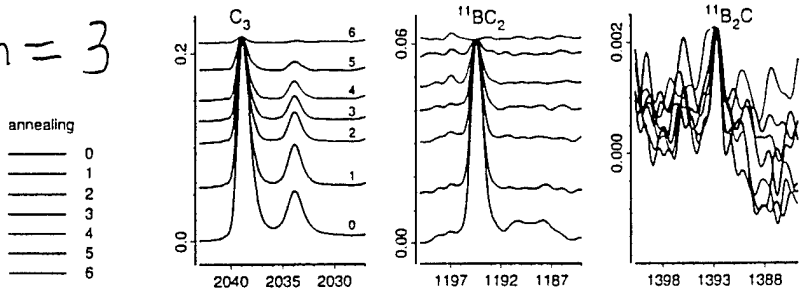

4

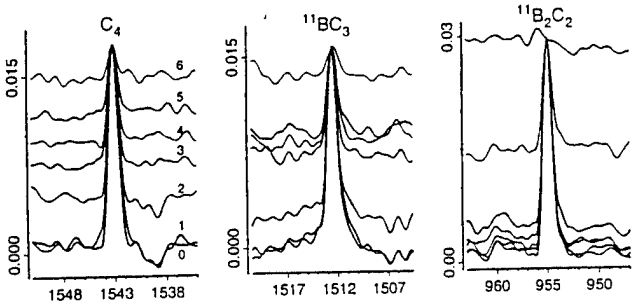

5

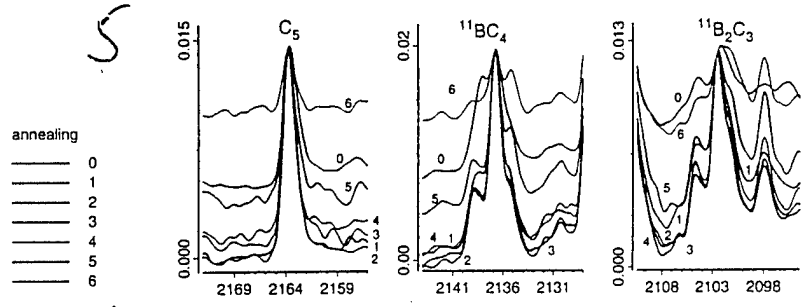

6

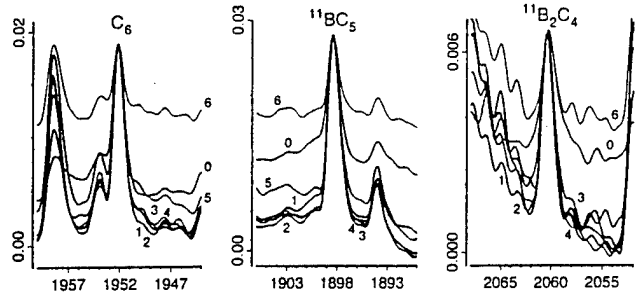

7

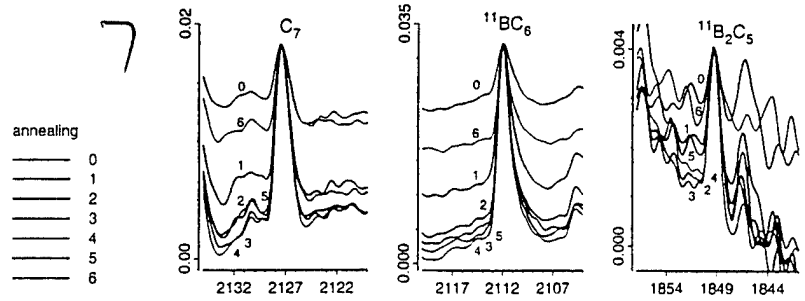

9

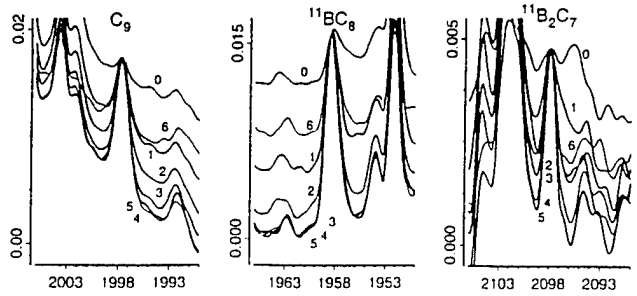

Conclusions

Linear C_3, cyclic BC_2, and cyclic B_2C, constituted about 80% of the total observable boron and carbon in the initially deposited matrix, but B_3 was not observed.

The measured trimer distribution in the initially formed matrices was

$$\rho(C_3) : \rho(BC_2) : \rho(B_2C) : \rho(B_3) \sim 1 : 1.5 : 0.5 : < 0.05.$$

Statistical substitution of J boron atoms into an n-atom carbon cluster produces a distribution given by $\rho(B_JC_{n-J})/\rho(C_n) = [\{n(n\text{-}1)\ldots(n\text{-}J\text{+}1)\}/J!]\ [B/C]^J$. With the experimental B/C ~ 1/3, the statistical trimer distribution is

$$\rho(C_3) : \rho(BC_2) : \rho(B_2C) : \rho(B_3) \sim 1 : 1 : 0.33 : 0.03.$$

Agreement between distributions implies trimers form by random condensation of well-mixed atoms, uninfluenced by the relative energies of the trimers, the energies of their precursors, or preferential kinetics pathways that could otherwise distort the statistics.

Linear C_3 and cyclic BC_2, disappeared entirely when the matrices were repeatedly annealed to temperatures between 25 K and 35 K, but cyclic B_2C was inert.

Linear C_4 and BC_3 (BCCC) disappeared more slowly, and linear B_2C_2 (BCCB) grew to ~ 95% of its final value during the first annealing. B_2C_2 was also inert, as B_2C.

The sources of B_2C_2 are from condensation of atom plus trimer ($B + BC_2$ but not $C + B_2C$) or dimer + dimer ($BC + BC$ but not $B_2 + C_2$). Although BC was not observed, the upper limit of $\rho(BC)$ is larger than $\rho(B_2C_2)$ so that BC cannot be ruled out as a source of B_2C_2.

The growth of B_2C_2 is conclusive evidence of the presence of BC and/or B in the originally deposited matrix in an amount at least as great as the growth of B_2C_2.

Linear C_5, BC_4 (BCCCC) and B_2C_3 (BCCCB)| and larger linear clusters (B_JC_{n-J}, $5 < n < 11$, $J = 0, 1, 2$), all grew upon annealing.

The sources of B_2C_3 are dimer + trimer ($BC + BC_2$ but not $B_2 + C_3$) and atom + tetramer ($B + BC_3$ but not $C + B_2C_2$).

Since $\rho(BC_2) \sim 5\rho(BC_3)$ in the initially deposited matrix, the $BC + BC_2$ source is dominant. Growth of B_2C_3 conclusively establishes the presence of BC in the matrix in an amount at least as great as the amount by which B_2C_3 grows.

Growth of BC_4 occurs primarily by $BC + C_3$ rather than $B + C_4$ or $C + BC_3$ because $\rho(C_3) \sim 10\rho(C_4)$ and $\rho(C_3) \sim 2\rho(BC_3)$. Growth of C_5 occurs by $C + C_4$ and $C_2 + C_3$, which establishes the presence of C and/or C_2 in the original matrix in an amount at least as great as C_5 growth.

Disappearance of triangular BC_2 requires breaking of one of its B-C bonds when one of its carbon atoms is attacked. The major reorganization of electronic energy involved in opening the ring appears to occur with little ($< \sim 3$ kcal mol^{-1}) or no energy barrier, which makes this small molecule a candidate for an interesting *ab-initio* study of unusual reactivity at low temperature.

Conclusions

1. C_3 is linear but BC_2, B_2C and B_3 are cyclic.

2. $n > 3$; $J = 0, 1, 2$ clusters are linear. Boron atoms cap the ends of linear chains.

3. $J = 0, 1, 2$ substitution in $n \geq 5$ clusters does not significantly affect IR intensities.

4. For $n \geq 5$ the absorption intensity of even n clusters is two to three times smaller than that of odd n clusters.

5. B_2C_2 grew most dramatically upon annealing. BC was not detected. Its upper limit column density is comparable to that of $n = 4$ clusters. B_2C_2 sources may be 2BC or $B + BC_2$ but $C + B_2C$ does not form B_2C_2.

6. $n = 3, 4$; $J = 0, 1$ clusters disappear upon annealing but $J = 2$ clusters either grow or remain unchanged. Capping the ends of clusters with boron seems to render them inert to further condensation.

7. Statistical cluster distributions are apparent in $n = 4$ and 5 clusters. B_2C yields are too high and B_2C_{n-2} yields are too low in larger $n \geq 6$ clusters.

8. $n \geq 5$ clusters grow upon annealing and larger clusters grow more than smaller clusters.

Conclusions from Carbon HEDM Research

Quantitative analysis - Establishes HEDM density, distribution of carbon clusters, heat of formation of HEDM. Enables tracking of growth and decay of carbon clusters - carbon bookkeeping - quantification of "invisible carbon", C-atom and C_2.

Highest density matrix (equivalent C-atom density ~ 1 mole percent in argon) contained 40% "invisible" carbon (C, C_2), determined by tracking the growth of the "visible" (measurable) carbon to a constant composition after repeated annealing. Main product of condensation is cyclic C_6.

Yields of cyclic-C_6 are a factor of two larger than the combined yield of all other clusters in the fully condensed, highest density matrices. Cyclic-C_6 is the dominant condensation product.

Knudsen oven produces ~ 80% C_3 and ~ 10% each of C_2 and C-atom (by mass).
Laval oven with $\Delta T \sim 600$ K (between graphite surface and orifice) produces ~ 5% C_3 and C_2 and ~ 90% C-atom. C-atoms production by our oven (relative to C_3) is enhanced by higher temperature, which is accompanied by higher ΔT.

Substrate must be shielded from oven to prevent condensation during deposition.
Higher temperature oven places higher heat load on substrate, which promotes condensation.

Obtained higher density matrices by decreasing argon flux and maintaining oven flux. However, condensation was also increased.

One experiment with argon/5% H_2 caused nearly complete loss of C_{n+1} and C_{n+2} relative to C_{n+3}, suggesting that H_2 scavenges C-atoms efficiently during co-deposition.